Development of Hybrid Organic-Inorganic Light Emitting Diodes Using Conducting Polymers Deposited by Oxidative Chemical Vapor Deposition Process

by

Hitesh Chelawat

Dual Degree (B. Tech & M. Tech)
Metallurgical Eng. and Materials Science (2007)
Indian Institute of Technology Bombay, Mumbai, India

Submitted to the Department of Materials Science and Engineering
in Partial Fulfillment of the Requirements for the Degree of
Master of Science in Materials Science and Engineering

at the

Massachusetts Institute of Technology

June 2010

Signature of Author: ..
Department of Materials Science and Engineering
May,2010

Certified by: .....
Karen K. Gleason
Professor of Chemical Engineering
Thesis Supervisor

Accepted by: .....
Krystyn J. Van Vliet
Associate Professor of Materials Science and Engineering
Thesis Reader

Accepted by: .....
Christine Ortiz
Professor of Materials Science and Engineering
Chair, Departmental Committee on Graduate Students

Development of Hybrid Organic-Inorganic Light Emitting Diodes Using Conducting Polymers Deposited by Oxidative Chemical Vapor Deposition Process

by

Hitesh Chelawat

Submitted to the Department of Materials Science and Engineering
on May 21'2010 in partial fulfillment of the
requirements for the Degree of Master of Science in
Materials Science and Engineering

ABSTRACT

Difficulties with traditional methods of synthesis and film formation for conducting polymers, many of which are insoluble, motivate the development of CVD methods. Indeed, conjugated polymers with rigid linear backbones typically crystallize readily and overcoming the resultant heat of crystallization makes them difficult to dissolve.

Poly(3,4-ethylenedioxythiophene) (PEDOT) thin films were obtained through oxidative chemical vapor deposition (oCVD) by using a new oxidant- bromine. The use of bromine eliminates any post processing rinsing step required with other oxidants like iron chloride and hence makes the process completely dry. Accelerated aging experiments show longer retention of electrical conductivity for the PEDOT films obtained using bromine as the oxidant. Conductivities as high as 380 S/cm were obtained for PEDOT films deposited using bromine as the oxidant at 80 °C, which is significantly higher than that for PEDOT films deposited using iron chloride as the oxidant at the same temperature. Cross-sectional SEM of the PEDOT films deposited using bromine on silicon trench wafers demonstrates high conformal deposition of the films. All the results show the possibility of depositing highly conducting, conformal PEDOT films on any substrate including silicon, glass, paper, plastic.

One of the many applications of conducting polymer is as hole-transport layer in light emitting diode. To be competitive in the LED market, improvements in hybrid-LED quantum efficiencies as well as demonstrations of long-lived HLED structures are necessary. In this work, we consider improvement in the stability of the HLED. The device fabricated can be configured as ITO/ Poly (EDOT-co-TAA)/CdSe (ZnS)/ Au. All the materials used in the device synthesis are stable in ambient conditions and all the synthesis steps on ITO substrate are done either in air or in very moderate pressure conditions. This significantly reduces the cost of the device fabrication by obviating the need of packaging layers and ultrahigh vacuum tools. The operating voltage as low as 4.3 V have been obtained for red-LEDs. We believe that with optimization of various layers in the device, further improvements can be made. For green LEDs we obtained the characteristic IV curve of a diode, but we still need to work on getting a functioning green LED.

Thesis Supervisor: Karen K. Gleason
Title: Professor of Chemical Engineering

Acknowledgment

I would like to extend my heartfelt gratitude and acknowledge the help of the following people for making this thesis, a reality.

I am heartily thankful to my advisor Karen Gleason, whose encouragement, supervision and support from the preliminary to the concluding level enabled me to develop an understanding of the subject. Her involvement with her originality has triggered and nourished my intellectual maturity that I will benefit from, for a long time to come. I am grateful to her in every possible way and hope to keep up our collaboration in the future.

I would also like to thank Professor Krystyn J. Van Vliet for being my thesis reader and giving her valuable time and insight.

My heartfelt thank to my lab group members with whom I shared the office and lab space. The variety of research carried out in this group is really mind boggling and I thoroughly enjoyed all the group meetings. I want to specially thank oCVD group- Miles, Rachel, Dhiman, Dave and particularly Sreeram Vaddiraju for teaching so much and being so helpful and considerate. Special thanks to Nathan for working on the business plan for this research work. In addition to my lab members, I would also like to thank Steven Kooi for helping out in the experiments in Institute for Soldier Nanotechnologies.

In MIT, learning experience is not restricted to lab and classroom only. I learned a lot from my fellow classmates, MIT Sangam community and board members, and Consulting club at MIT members. I want to thank all of them for enriching my life. Special thanks to my friends – Vaibhav, Shreerang, Prithu, Naveen, Mehul, Asha and others who remain unnamed for making my stay in MIT so wonderful.

A lot has happened in the course of the two years of my stay in MIT. I got engaged to Mahima and her endless love and support has really helped me in sailing through everything. My special gratitude is due to all my family members for their loving support.

Needless to say this journey wouldn't have been possible without the support of my parents and my sweet sister Ragini. Their continuous motivation, prayers for my success and belief in me played a big role. I will always be grateful to them.

Thank you almighty for blessing me with the support and love of such exceptional individuals! I owe it all to you.

TABLE OF CONTENTS

List of Figures

CHAPTER THREE

Chapter One

Introduction

M. E. Alf, Dr. A. Asatekin, M. C. Barr, Dr. S. H. Baxamusa, **H. Chelawat**, Dr. G. Ozaydin-Ince, C. D. Petruczok, Dr. R. Sreenivasan, Dr. W. E. Tenhaeff, N. J. Trujillo,Dr. S. Vaddiraju, J. J. Xu, K. K. Gleason, 'Chemical Vapor Deposition of Conformal, Functional,and Responsive Polymer Films', ***Adv. Mater.*** **2009**, 21, 1–35

1.1 Conducting Polymers

Since their discovery in 1970[1], extensive research on conducting polymers has been motivated by potential applications for flexible electronic devices including light emitting diodes (LEDs), transistors, biosensors, biomedical devices, chemical sensors, solar cells, electrodes, microwave absorbing materials, new types of memory devices, nanoswitches, optical modulators and valves, imaging materials, polymer electronic interconnects, nanoelectronic and optical devices and nonlinear optical devices [2-9]. Conducting polymers show negligible conductivity in the neutral state. Conductivity results from the formation of charge carriers upon oxidation or reduction of their conjugated backbone[10-12].

Difficulties with traditional methods of synthesis and film formation for conducting polymers, many of which are insoluble, motivate the development of CVD methods. Indeed, conjugated polymers with rigid linear backbones typically crystallize readily and overcoming the resultant heat of crystallization makes them difficult to dissolve[13]. Electrochemical synthetic methods produce films of poly (3, 4-ethylenedioxythiophene) (PEDOT) with conductivities as high as 300 S/cm[14] but this method is only compatible with conducting substrates[5]. Wet chemical oxidative polymerization from solutions containing oxidants like $Fe(III)Cl_3$ or Fe(III) p-toluenesulfonate (Fe(III) tosylate) results in PEDOT films of similar conductivity. Films result from either casting the reaction mixture onto a surface or allowing the solvent to evaporate or by immersing substrates directly in the reaction mixture[15, 16]. These chemical routes are applicable to a wider range of substrates but can suffer from lack of reproducibility[17].The incorporation of the soluble solid state dopant, polystyrenesulphone

(PSS) in an aqueous emulsion of PEDOT:PSS, enables spin casting of composite films (commercial name of Baytron P). However, the incorporation of PSS lowers conductivity to < 10 S/cm [18].

A variety of deposition methods have been devised for the vapor phase introduction of the monomer into a vacuum chamber where polymerization and film formation occurs in single step at the growth surface. The CVD methods are often compatible with substrates as fragile as paper [19, 20]. PECVD has been used in conjunction with thiophene (and its derivatives) [21-32], pyrrole[19, 29, 33] and aniline [34-36] monomer. Both the chemical structure and properties of the PECVD films differ from the conducting polymers obtained by traditional wet synthetic methods and are dependent on the plasma polymerization conditions. For thiophene and its derivatives, coatings obtained by PECVD have very low or even no conductivity, most likely due to the loss of aromatic structure or thiophene ring being opened during the energetic and chemical non-selective plasma polymerization process[21, 23, 25]. Sadhir et al. prepared plasma polymerized thiophene layers using argon as an initiator and after overnight doping with iodine found conductivities ranging from 10^{-6} to 10^{-4} S/cm. Retention of the ring structure in the films was enhanced by performing the growth downstream of the plasma discharge region[23]. Giungato et al. carried out in-situ doping by using a mixture of argon, thiophene and iodine. Although fragmentation does occur, the thiophene ring was preserved to some extent and a conductivity of 10^{-5} S/cm was obtained without additional doping[37]. PECVD at atmospheric pressures results in higher preservation of the conjugation of thiophene and its derivatives with conductivities up to 1×10^{-2} S/cm [28, 38]. Pulsed PECVD also increased the retention of intact conjugated rings in the films grown from pyrrole and

thiophene[39]. For thiophene, pulsed PECVD resulted in transparent films >80% with conductivities of ~10^{-5} S/cm [21]. The conductivity of PECVD films from tetracyanoquinodimethane was observed to increase substantially to 10^{-5} S/cm from 10^{-9} S/cm with the addition of quinoline[40]. Griesser et. al. demonstrated variation in the chemical and physical characteristics of the PECVD films deposited from aniline with discharge conditions. The optimized films prepared were smooth and free of solvent and oxidant suggesting better physical properties than those obtained by wet chemical methods [35].

Vapor phase polymerization (VPP) directly translates the step-growth mechanism established for the wet synthesis conducting polymers to a solvent-less environment. As early as 1986, Mohammadi et al. obtained polypyrrole films by supplying vapors of both the oxidant (iron chloride) and the monomer (pyrrole) onto substrates maintained at a temperature of 0 °C. The conductivity of the samples obtained ranged from 10^{-2} to 1 S/cm [41].

The VPP method to produce conducting polymers like polypyrrole and PEDOT has been reported by Kim et al. [42, 43] using $FeCl_3$ as oxidant. Rather than being delivered through the vapor phase, the $FeCl_3$, which is a low volatility solid under ambient conditions, was pre-applied to the substrate by a dip or a micro gravure roll coating method. The monomer was subsequently delivered through the vapor phase. The maximum conductivity of PEDOT obtained by this method was 70 S/cm. Winther-Jensen et al. further improved the conductivity by using base-inhibited (pyridine) VPP of EDOT and reported conductivities as high as 1025 S/cm for a film thickness of 250 nm [44]. Winther-Jensen et al. also accomplished deposition of polypyrrole and PEDOT using iron

sulfonate as an oxidizing agent[45] and successfully depositing optically active polyaniline[46]. In some cases, PEDOT prepared by VPP has shown better performance than those prepared by wet methods. For example photovoltaic devices with VPP PEDOT showed higher short circuit current and better fill factor than one fabricated with spin coated PEDOT:PSS [47] and an air electrode based on a porous material coated by VPP PEDOT showed higher oxygen reduction potential because of more stability, improved ordering in this method[48]. Researchers have also used VPP PEDOT as electrode because of its low work function (~ 4 - 4.5 eV) and high conductivity ($10^2 - 10^3$ S/cm) [49, 50].

VPP has been employed to direct the formation of polypyrrole on selected areas of a substrate. Chlorine treatment of patterned metal film, followed by exposure to pyrrole monomer vapor was employed for obtaining submicron-wide conducting polymer films in this report [51]. Polypyrrole film was only observed on the areas containing the metal at the end of the experiment as these are the only areas having metal chloride available for polymerizing the pyrrole monomer. A strategy of exposing iron chloride treated substrates[24, 47], porous templates[52] and cellulose fibers[53] to pyrrole vapor resulted in the successful formation of polypyrrole films, nanotubes and textiles, respectively.

Another strategy, oxidative chemical vapor deposition (oCVD), was developed by Gleason and coworkers for the synthesis of a number of conducting polymers, including poly(3,4-ethylenedioxythiophene) PEDOT, Polypyrrole (PPY), poly(3-thiopheneacetic acid) (PTAA) and copolymers like poly(EDOT-co-TAA), poly(pyrrole-co-TAA)[20, 54-65]. Analogous to the early work by Mohammadi *et.al* [41], both the oxidant and commercially available monomers are delivered directly to the substrate in the vacuum chamber

through the vapor phase [55]. High rate oCVD growth is enabled by utilizing a high flux of oxidant, typically created by a heated crucible internal to the vacuum chamber, and by utilizing monomer partial pressures which are significant relative to the vapor pressure of the monomer. PEDOT films with thicknesses more than 200 nm are formed in 30 min[56]. The in situ vapor phase delivery of the oxidant distinguishes oCVD from VPP processes that pre-apply oxidant before placing the substrate in the vacuum chamber. In oCVD it is possible to do continuous film growth by simultaneously flowing the oxidant and the monomer to the substrate. However oxidant can also be in-situ delivered to the substrate before the monomer, to give self limited growth of the polymer film similar to VPP. Smooth oCVD PEDOT films with conductivities as >1000 S/cm has been obtained[57]. Furthermore, independent control over the substrate temperature permits systematic variation in film properties including the tuning of work function and conductivity of the oCVD PEDOT films. The conductivity was found to increase with increase in temperature, with activation energy of 28.2 ± 1.1 kcal/mol, attributed to the formation of chains of increased conjugation length during growth at higher substrate temperatures[56]. Work function changed from 5.1 to 5.4 eV as the substrate temperature varied from 15 to 100 ^{o}C [58]. This ability to tune the work function is important for optimizing device performance, including the fabrication of efficient photovoltaic cells. Electrochromic devices fabricated using 100 nm thick oCVD PEDOT films on ITO/glass displayed optical switching speeds of 13 and 8.5 s for light-to-dark and dark-to-light transitions, respectively. The color contrast was 45% at 566 nm and is 85% stable over 150 redox cycles[59]. The compatibility of oCVD deposition of PEDOT has been demonstrated on glass, silicon, plastic and paper substrates[20]. Additionally, the morphology of oCVD films

depends upon the oxidizing agent. For instance, $FeCl_3$ results in smooth films with an RMS roughness of 4 nm whereas use of the weaker oxidant $CuCl_2$ results in films with a basalt-like nanoporous morphology [60].

Patternability is a key for integrating conducting polymers into electronic circuits and requires excellent adhesion of the conducting polymer to the substrate. The oCVD method enables the systematic ability to graft conducting polymers to substrates[61]. The oxidant, $FeCl_3$, is a Friedel-crafts catalyst which simultaneously creates radical cations on the monomer and on substrate, provided the substrate contains aromatic groups. Indeed, oCVD PEDOT films covalently attach to polystyrene, polyethyleneterephthalate, polycarbonate, polyethylenenaphthalate, polyurethane, and poly(acrylonitrile-butadiene-styrene) substrates[61] . The adhesion provided by grafting enables the resolution of 60 nm features of oCVD PEDOT on flexible polyethyleneterephthlate substrates. Extending this concept, silane coupling agents containing aromatic groups enable the grafting of PEDOT on silicon and glass and facilitate subsequent patterning on these substrates.

The oCVD process also enables introduction of functional groups in conducting polymer films using commercially available monomers, for instance through the copolymerization of pyrrole with thiophene-3-acetic acid[62]. This copolymerization scheme allowed for tuning both the amount of –COOH functionality and the conductivity of the resulting oCVD films. The presence of –COOH functional groups allowed the subsequent uniform assembly of metal nanoparticles through covalent bonding to the films for obtaining conducting polymer-metal nanoparticle hybrids. An interesting result observed was that the conductivity of the resulting hybrids depended on the type of linker molecule employed for the assembly and use of conjugated linker molecule (e.g. 4-

aminothiophenol) resulted in an enhancement of the resulting hybrids[62, 63]. Similar strategy was also employed to assemble quantum dots on conducting polymer films for the fabrication of hybrid light emitting diodes[64]. Recently a method for the fabrication of composites by conformal coating of aligned CNTs arrays by conducting polymer through the oCVD process was developed. It was observed that the oCVD process preserves the morphology and structure of CNT arrays. In addition to enhancing the conductivity, this process allowed for exploiting the directional dependant properties of the composites [65].

Additionally, VDP synthesis enables the deposition of electroluminescent semiconducting polymers, including poly (2,5-thienylene vinylene) (PTV)[66] and poly(phenylene vinylene) (PPV) [67, 68]. As early as 1989, the pyrolysis of [2.2] (2,5) thiophenophane vapors were employed for the formation of poly(2,5-thienylene-ethylene) (PTE). Oxidation of this insoluble PTE film led to the formation of fully conjugated PTV films[66]. Iwatsulki and coworkers employed VDP of 1,9-dichloro [2.2] paracyclophane for obtaining conjugated PPV film. The presence of chlorine in the precursor monomer allowed for its easy dissociation in this case[67]. Similarly, pyrolysis followed by condensation of mono- and di- substituted α,α'-Dichloro-*p*-xylenes was also reported to lead to the formation of PPV films[68, 69]. CVD of copolymers of PPV and parylene using α,α'-Dichloro-*p*-xylenes and [2.2] paracyclophane for the formation of blue electroluminescent polymers was also reported by Jensen and coworkers[70].

We have obtained Poly(3,4-ethylenedioxythiophene) (PEDOT) thin films through oxidative chemical vapor deposition (oCVD) by using a new oxidant- bromine[71]. The use of bromine eliminates any post processing rinsing step required with other oxidants like iron chloride and hence makes the process completely dry. Film properties are further

compared with the PEDOT films deposited using iron chloride as the oxidant. Accelerated aging experiments shows longer retention of electrical conductivity for the PEDOT films obtained using bromine as the oxidant. Conductivities as high as 380 S/cm were obtained for PEDOT films deposited using bromine as the oxidant at 80 °C, which is significantly higher than that for PEDOT films deposited using iron chloride as the oxidant at the same temperature. Cross-sectional SEM of the PEDOT films deposited using bromine on silicon trench wafers demonstrates high conformal deposition of the films. All the results show the possibility of depositing highly conducting, conformal PEDOT films on any substrate including silicon, glass, paper, plastic.

1.2 Light Emitting Diodes

A light emitting diode (LED) is basically a semiconductor diode which emits light when it is forward biased. The source of light is the combination of electron and hole within the device, releasing energy in the form of photons. The color of the light is determined by the energy gap of the semiconductor and the effect is called electroluminescence. The working principle of a typical LED is shown in the Fig. 1-1 below[72]: -

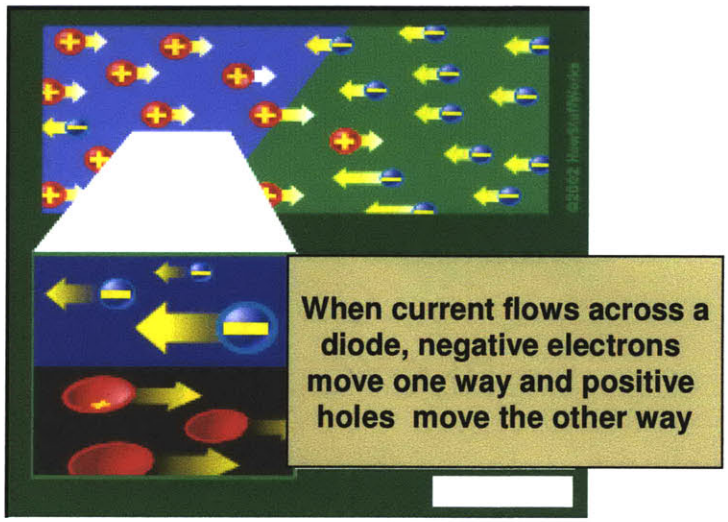

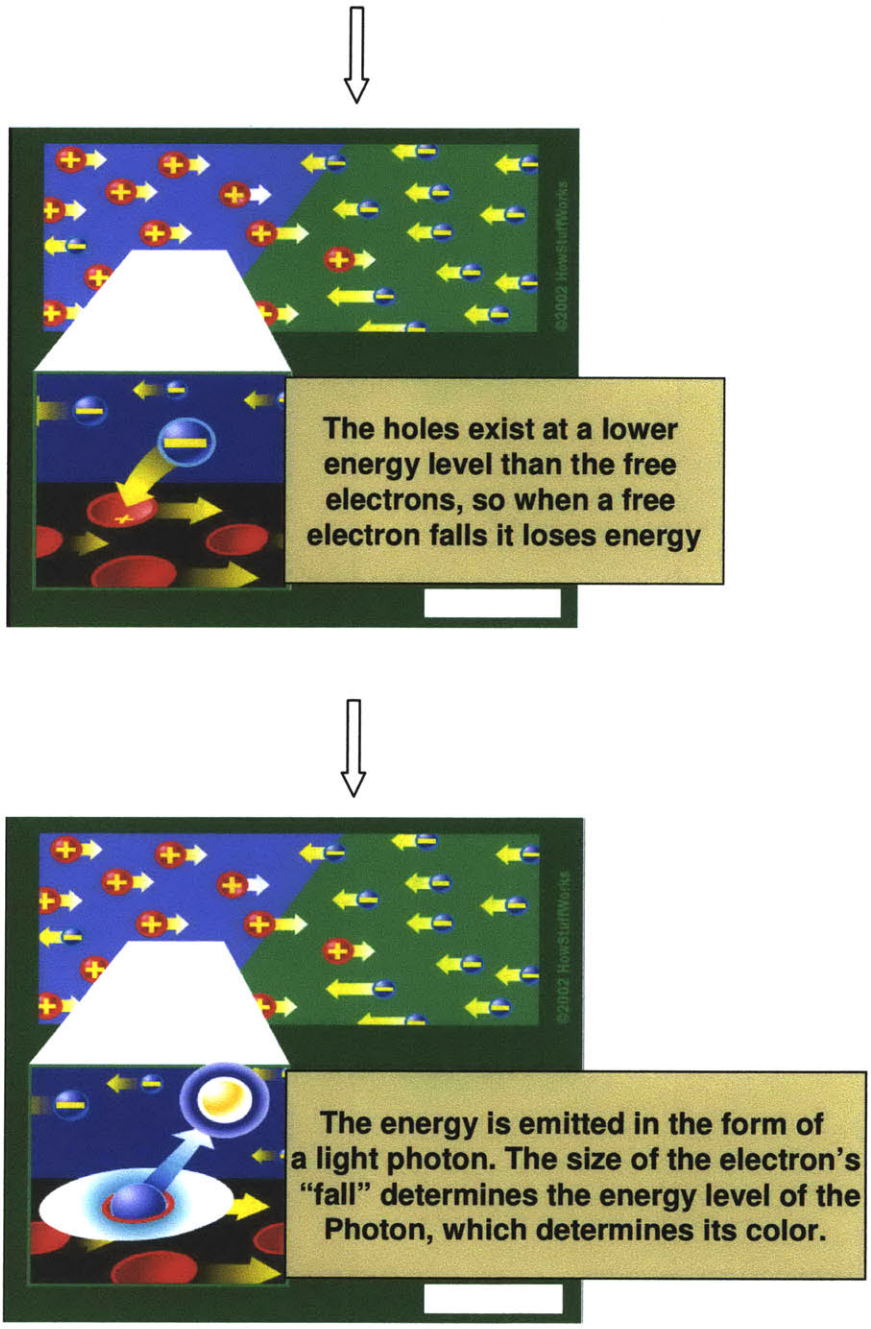

Figure 1-1: Working principle of a typical LED[72]

LED's present many advantages over incandescent light sources as listed below: -

- Higher efficiency
- Smaller size

- Faster switching
- Greater durability and reliability
- Longer lifetime
- Higher shock resistance

But the biggest disadvantage of LED over traditional lighting source is its high initial cost. Various types of LED's are manufactured depending upon the cost and the requirement of application. For example inorganic LED's, organic LED's, polymer LED's. Organic LED's are lighter where as polymer LED's can be made on flexible substrate.

1.2.1 Quantum Dots (QDs) Based Hybrid Organic Inorganic LED's (HLED)

Hybrid structures consisting of semiconducting organic polymers and strongly luminescent nanocrystals offer advantages like highly saturated, tunable emission and tunable absorption, in combination with an easy processibility from solution and low materials cost[73]. The advantage of using quantum dots(QDs) in HLED include high chemical and optical stabilities, easy tuning of the saturated color emission across the visible-NIR range, and easy processibility in hybridizing organic and inorganic materials. Also modification of surface ligands of QDs increases the QDs luminescence efficiency and their flexibility in diverse applications.

In 1994, Colvin et al.[74] reported first HLED based on a bi-layer device comprising a thin layer of CdSe nanocrystals deposited on a conducting support, comprised of ITO, with the help of an aliphatic linker hexane dithiol, and a 100 nm thick layer of a soluble PPV derivative. The nanocrystals were dissolved in toluene and solution was exposed to either ITO or ITO/PPV treated with hexane dithiol, a bi-functional compound which binds nanocrystals to the surfaces. The structure was sandwiched in between an ITO-

coated glass and an Mg/Ag electrode, which functioned as anode and cathode, respectively. This device showed the emission characteristic of CdSe nanocrystals with an operating voltage of 4 V only, with an EL band tunable from yellow to red by changing nanocrystals size.

Rubner et al.[75] reported a single-layer device where CdSe nanocrystals were homogeneously distributed with in a polymer layer of polyvinylcarbazole as hole conducting component, which additionally contained an oxidiazole derivative (butyl-PBD) as an electron transporting molecular species. The resulting volume fraction of CdSe nanocrystals in a film sandwiched between ITO and Al electrodes was 5-10 %, below the percolation threshold for charge transport to occur between the nanocrystals. The photoluminescence and electroluminescence spectra of the devices were reasonable narrow with FWHM < 40 nm and were tunable from 530 nm to 650 nm by varying the size of the nanocrystals. Following work on bi-layer devices based on core-shell nanocrystals has shown sufficient improvements over the core-only CdSe-based devices, namely a factor of 20 increase in efficiency to 0.22% and a factor of 100 in lifetime in air under constant current to several hours and operating voltages as low as 4V[76, 77].

Tri-layer hybrid nanocrystal/organic molecule LEDs[78] with a single monolayer of CdSe/ZnS nanocrystals sandwiched between two organic thin films were designed in 2002. This device showed an external quantum efficiency of more than 0.4% for a broad range of luminance with brightness of as 2000 cd m^{-2} at 125 mA cm^{-2}.

Hybrid LEDs with layer by layer assembly was first built by Gao et al. using 20 alternating double layers of a precursor of PPV and CdSe nanocrystals capped by thiolactic acid. This device emitted white light originating mainly from recombination

through nanocrystal trap sites, a turn on voltage between 3.5 – 5 V and an external quantum efficiency of 0.0015%[79]. Electroluminescence of different colors from green to red was obtained in layer-by-layer assembled LEDs by using thioglycolic acid capped CdTe nanocrystals of different sizes and poly (diallyldimethylammonium chloride) (PDDA)[80]. Light emission was observed in these assembly devices at an onset voltage of 2.5 – 3.5 V with current densities of 10 mA cm^{-2}.

A detailed hybrid LED device fabricated using quantum dots is shown in the Fig. 1-2[81]. The device configuration can be depicted as ITO/PEDOT:PSS/poly-TPD/QD/BCP/Alq_3/LiF/Al. Poly(3,4-ethylenedioxythiophene)-poly(styrenesulfonate) (PEDOT-PSS) and a poly(N,N'-bis(4-butylphenyl)-N,N'-bis(phenyl) benzidine) (poly-TPD) were used as the hole transport layer whereas the 2,9-dimethyl-4,7-diphenyl-1,10-phenanthroline (BCP) and tris(8-hydroxyquinoline) aluminium (Alq_3) were used as the electron transport layers. BCP also acts an a hole blocking layer so it greatly enhance the probabilities of electron and hole injection into the QDs. The maximum brightness for this device was 141 cd m^{-2} at 11.5 V.

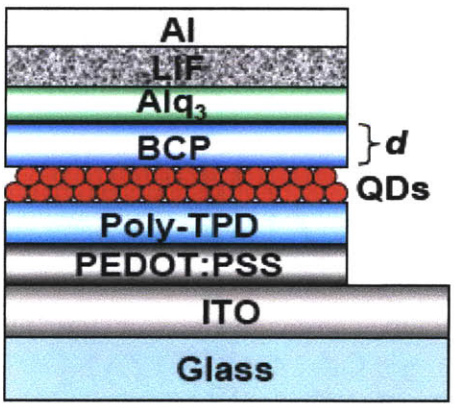

Figure 1-2: A schematic diagram of the device configured as ITO/PEDOT:PSS/poly-TPD/QD/BCP/Alq_3/LiF/Al.. The thickness'd' of the BCP layer is varied from 0-30 nm[81].

Gigli et al.[82] fabricated HLED using stable red-emitting CdSe/ZnS core-shell quantum dots covered with a trioctylphosphine oxide organic ligand doped in a polymer layer. Active layer in the device consisted of blue-emitting poly[(9,9-dihexyloxyfluoren-2,7-diyl)-alt-co-(2-methoxy-5-(2-ethlyhexyloxy)phenylen-1,4-diyl)] (PFH-MEH) doped with red-emitting QDs and a green emitting metal chelate complex Alq_3. These devices had external quantum efficiency of 0.24% at 1 mA cm^{-2} at 11 V in air. Bulovic etal.[83] demonstrated the applicability of phase segregation process in the fabrication of QD-LEDs containing a wide range of CdSe particle sizes (32 Å to 58 Å). By varying the size of QDs, peak electroluminescence was varied from 540 nm to 653 nm. The energy diagram of the device manufactured is shown in the Fig. 1-3.

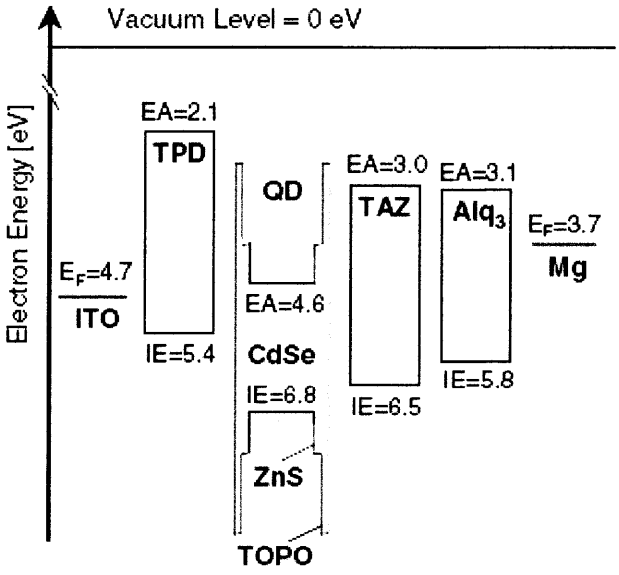

Figure 1-3: Energy diagram for QD-LEDs. The highest occupied molecular orbital (HOMO) and lowest unoccupied molecular orbital (LUMO) band energies were determined from photoemission spectroscopy and inverse photoemission spectroscopy measurements[83].

Lee et al. studied the effect of incorporation of QDs into a semiconducting polymer and observed that nanoparticles enhanced the working of HLED by acting as charge carriers, electro-optical active centers, or optical microcavities[84]. The configuration of the device fabricated was ITO/PEDOT/CdSe(ZnS) and polymer blend/Ca/Al. For pure polymer device emitting yellow light, maximum brightness of 3949 cd m^{-2} and maximum external quantum efficiency of 0.27 cd A^{-1} at 10 V was obtained. After blending with CdSe(ZnS) QDs device showed much improved performance with maximum brightness as high as 8192 cd m^{-2} with maximum external quantum efficiency of 1.27 cd A^{-1} at 7 V.

Electroluminescence from a mixed red-green-blue colloidal QD monolayer was studied by Anikeeva et al.[85]. Colloidal QDs were reproducibly synthesized and yield high luminescence efficiency materials suitable for LED applications. Precise tuning of the emission spectrum without changing of the device structure was materialized by changing the ratio of different colors QDs in the active layer. Independent processing of the organic charge transport layers and the QD luminescent layer allowed fine spectral tuning of the device with white HLED exhibiting external quantum efficiency of 0.36%.

A solvent-free contact printing process for patterned and unpatterned colloidal QD thin films was demonstrated by Kim et al.[86].This simple, low cost, high throughput method eliminates the exposure of the device structures to solvents. The charge transport layers in HLED consists of a solvent-sensitive organic thin films, the ability to avoid solvent exposure during device growth provides lot of flexibility in choosing organic materials to improve device performance. The four step contact printing process is shown in the Fig. 1-4: -

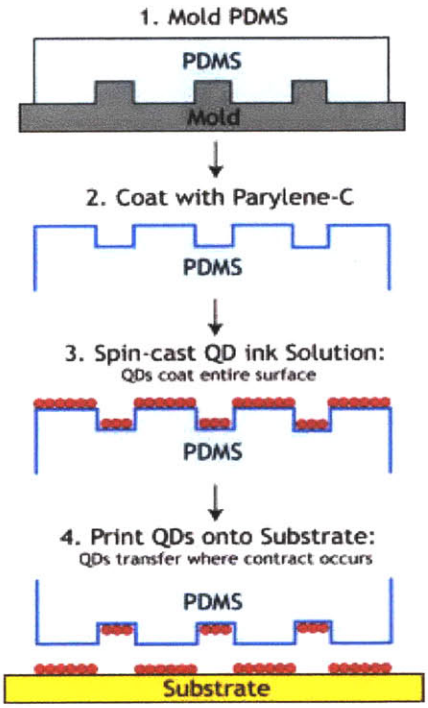

Figure 1-4: Schematic showing the four step solvent free contact printing process for QDs.

1.3 Scope of Thesis

Chapters two and three are structured as journal articles, each containing independent introduction, experimental methods, results and discussion, and chapter conclusions. Although each of these chapters can be read as independent work, there is a connection between the two chapters.

In Chapter two, we present a completely dry oxidative chemical vapor deposition process to deposit conducting polymers. Results presented in the chapter show that application of bromine as the oxidant improves the conductivity and stablility of the PEDOT films deposited. Conformality, conductivity, chemical bonding, elemental composition is compared with the PEDOT films deposited using iron chloride as the oxidant.

Chapter three reports a novel technology developed to fabricate hybrid light emitting diodes. Unlike other processes employed in making HLED, our method does not involve use of oxidizable organic layers like PPV or use of ultrahigh vacuum tools to deposit any of the layers. All starting materials used are stable in ambient conditions and the covalent interfacing of different layers in the HLED results in a robust interface. For hole-transport layer in our device, we deposited conducting polymer layer using oxidative chemical vapor deposition (oCVD) process which is a completely dry, solvent free method with no requirement for ultrahigh vacuum tools. Water soluble QDs were further attached to the conducting polymers using a linker molecule. The device structure was sandwiched between ITO and a metal electrode-gold. The series of steps required for device fabrication can be carried our in air or very moderate vacuum conditions. Preliminary results are very promising for the development of stable, efficient hybrid light emitting diodes.

Chapter four contains the conclusions for the previous sections and discusses the directions for future work.

Work in Chapter two was supported by Eni S.p.A. under the Eni-MIT Alliance Solar Frontiers Program. The funding for the work reported in Chapter three was provided by the Deshpande Center at MIT.

1.4 References

1. A. J. Heeger, *Journal of Physical Chemistry* 2001, Vol. 105, No. 36, 8475.
2. J. H. Burroughes, D. D. C. Bradley, A. R. Brown, R. N. Marks, K. Mackay, R. H. Friend, P. L Burns, A. B. Holmes, *Nature* 1990, 347, 539.
3. H. E. Katz, *Journal of Material Chemistry* 1997, 7, 369.
4. M. Gerard, A. Chaubey, B. D. Malhotra, *Biosensors and Bioelectronics* 2002, 17, 345.
5. N. K. Guimard, N. Gomez, C. E. Schmidt, *Progress in Polymer Science* 2007, 32, 876.
6. U. Lange, N. V. Roznyatovskaya1, V. M. Mirsky, *Analytica Chimica Acta* 2008, 614, 1.
7. M. Angelopoulos, *IBM J. RES. & DEV.* 2001, Vol. 45 No. 1, 57.
8. H. Hoppe, N. S. Sariciftci, *Journal of Materials Research* 2004, Vol. 19, No. 7, 1924.
9. A. Moliton, R. C. Hiorns, *Polymer International* 2004, 53, 1397.
10. J.L. Bredas, G.B. Street, *Accounts of Chemical Research* 1985, 18, 309.
11. P. Chandrasekhar, *Conducting Polymers, Fundamentals and Applications: A Practical Approach, Springer* 1999, 35.
12. Perfluorinated Polymers. Kirk-Othmer Encyclopedia of Chemical Technology; John Wiley & Sons, Inc., 2004, 18, 1.
13. G. H. Chen, M. Gupta, K. Chan, K. K. Gleason, *Macromol. Rapid Commun.* 2007, 28, 2005.

14. Yamato, H.; Kai, K.; Ohwa, M.; Asakura, T.; Koshiba, T.; Wernet, W., *Synth. Met.* 1996, 83, 125.

15. Hohnholz, D.; MacDiarmid, A. G.; Sarno, D. M.; Jones, W. E., *Chem. Commun.* 2001, 2444.

16. Tran-Van, F.; Garreau, S.; Louarn, G.; Froyer, G.; Chevrot, C.; *J. Mater. Chem.* 2001, 11, 1378.

17. Winther-Jensen, B.; Breiby, D. W.; West, K. *Synth. Met.* 2005, 152, 1.

18. Jonas, F.; Morrison, J. T. *Synth. Met.* 1997, 85, 1397.

19. H. T. Sahin, *Central European Journal of Chemistry* 2007, 5(3), 824

20. J. P. Lock, S. Im, K. K. Gleason, *Macromolecules* 2006, 39, 5326.

21. L. M. H. Groenewoud, G. H. M. Engbers, J. G. A. Terlingen, H. Wormeester, J. Feijen, *Langmuir* 2000, *16,* 6278.

22. N. V. Bhat, D. S. Wavhal, *Journal of Applied Polymer Science* 1998, 70, 203.

23. R. K. Sadhir and K. F. Schoch, *Thin Solid Films* 1993, 223, 154.

24. M. S. Silverstein, I. Visoly-Fisher, *Polymer* 2002, 43, 11.

25. L. M. H. Groenewoud, G. H. M. Engbers, and J. Feijen, *Langmuir* 2003, *19,* 1368

26. K. Tanaka, K. Yoshizawa, T. Takeuchi, T. Yamabe, *Synthetic Metals* 1990, *38,* 107.

27. M. E. Ryan, A. M. Hynes, S. H. Wheale, and J. P. S. Badyal, *Chem. Mater.* 1996, *8,* 916.

28. R. Dams, D. Vangeneugden, D. Vanderzande, *Chem. Vap. Deposition* 2006, *12,* 719.

29. J. G. Wang, K.G. Neoh, E.T. Kang, *Thin Solid Films* 2004,446, 205.

30. B. Winther-Jensen, K. Norrman, P. Kingshott, K. West, *Plasma Process. Polym.* 2005, 2, 319.

31. E. Vassallo, L. Laguardia, M. Catellani, A. Cremona, F. Dellera, F. Ghezzi, *Plasma Process. Polym.* 2007, 4, S801.

32. T. W. Kim, J. H. Lee, J. W. Back, W. G. Jung, J. Y. Kim, *Macromolecular Research* 2009, 17, V1, 31.

33. J. L. Yague, N. Agullo, S. Borros, *Plasma Process. Polym.* 2008, 5, 433.

34. P. A. Tamirisa, K. C. Liddell, P. D. Pedrow, M. A. Osman, *Journal of Applied Polymer Science* 2004, Vol. 93, 1317.

35. X. Gong, L. Dai, A. W. H. Mau, H. J. Griesser, *Journal of Polymer Science: Part A: Polymer Chemistry* 1998, 36, 633.

36. U. S. Sajeev, C. J. Mathai, S Saravanan, R. R. Ashokan, S. Venkatachalam, M. R. Anantharaman, *Bull. Mater. Sci.* 2006, 29- 2, 159.

37. Giungato, P.; Ferrara, M. C.; Musio, F.; d'Agostino, R. *Plasmas Polym.* 1996, *1*, 283.

38. K. Tanaka, S. Okazaki, T. Inomata, M. Kogoma, *Thin Solid Films.* 2001, 386-2, 200.

39. L. Martin, J. Esteve, S. Borros, *Thin Solid Films* 2004, 451-452, 74.

40. X. Xie, J. U. Thiele, R. Steiner and P. Oelhafen, *Synthetic Metals* 1994, 63, 221.

41. A. Mohammadi, I. Lundstro¨ m, W.R. Salaneck, O. Inganas, *Chemtronics* 1986, 1, 171.

42. J. Kim, D. Sohn, Y. Sung, E.R. Kim, *Synth. Met.* 2003, 132, 309.

43. J. Kim, E. Kim, Y. Won, H. Lee, K. Suh, *Synth. Met.* 2003, 139-2, 485

44. B.W. Jensen, K. West, *Macromolecules* 2004, 37, 4538.

45. B.W. Jensen, J. Chen, K. West, G. Wallace, *Macromolecules* 2004, 37, 5930.

46. J. Chen, B. W. Jensen, Y. Pornputtkul, K. West, L. K. Maquire, G. G. Wallacea, *Electrochemical and Solid-State Letters* 2006, 9(1), C9.

47. S. Admassie, F. Zhang, A.G. Manoj, M. Svensson, M. R. Andersson, O. Inganas, *Solar Energy Materials & Solar Cells* 2006, 90, 133.

48. B. W. Jensen, O. W. Jensen, M. Forsyth, D. R. MacFarlane, *Science* 2008, 321, 671.

49. A. Gadisa, K. Tvingstedt, S. Admassie, L. Lindell, X. Crispin, M. R. Andersson, W.R. Salaneck, O. Inganas, *Synthetic Metals* 2006, 156, 1102.

50. L. Lindell, A. Burquel, F. L. E. Jakobsson, V. Lemaur, M. Berggren, R. Lazzaroni, J. Cornil, W. R. Salaneck, X. Crispin, *Chem. Mater.* 2006, *18,* 4246

51. F. Cacialli, P. Bruschi, *J. Appl. Phys.* 1996, 80, 70.

52. J. Jang, J. H. Oh, *Chemical Communications* 2004, 882.

53. L. Dall'Acqua, A. Varesano, M. Canetti, W. Porzio, M. Catellani, *Synthetic Metals* 2006, 156, 379.

54. W. E. Tenhaeff, K. K. Gleason, *Advanced Functional Materials* 2008, 18, 979.

55. S. Im, K. K. Gleason, *Macromolecules* 2007, 40, 6552.

56. S. G. Im, E. A. Olivetti, K. K. Gleason, *Surface Coatings and Technology* 2007, 201, 9406.

57. S. H. Baxamusa, S. G. Im, K. K. Gleason, *Phys. Chem. Chem. Phys.* 2009, 11, 5227

58. S. G. Im, K. K. Gleason and E. A. Olivetti, *Appl. Phys. Lett.* 2007, 90, 152112.

59. J. P. Lock, J. L. Lutkenhaus, N. S. Zacharia, S. G. Im, P. T. Hammond, K. K. Gleason, *Synthetic Metals* 2007, 157, 894

60. S. G. Im, D. Kusters, W. Choi, S. H. Baxamusa, M. C. M. V. D. Sanden, K. K. Gleason, *ACS Nano* 2008, 2-9, 1959.

61. S. Im, P. J. Yoo, P. T. Hammond, K. K. Gleason, *Advanced Materials* 2007, 19, 2863.

62. S. Vaddiraju, K. Senecal, K. K. Gleason, *Advanced Functional Materials* 2008, 18, 1929

63. Vaddiraju, S.; Gleason, K. K.,*Nanotechnology* 2010, 21, (12), 1.

64. S. Vaddiraju, K. K. Gleason, *Manuscript in Preparation* 2009.

65. S. Vaddiraju, H. Cebeci, B. L. Wardle, K. K. Gleason, *Manuscript in Preparation* 2009.

66. S. Iwatsuki, M. Kubo, H. Yamashita, *Chemistry Letters* 1989, 729.

67. S. Iwatsuki, M. Kubo, T. Kumeuchi, *Chemistry Letters* 1991, 1071.

68. E.G.J. Staring, D. Braun, G.L.J.A. Rikken, R.J.C.E. Demandt, Y.A.R.R. Kessener, M. Bouwmans, D. Broer, *Synthetic Metals* 1994, 67, 71.

69. A. K. Li, N. Janarthanan, C. S. Hsu, *Polymer Bulletin* 1991, 45, 2000.

70. K. M. Vaeth, K. F. Jensen, *Macromolecules* 2000, 33, 5336.

71. H. Chelawat, S. Vaddiraju, K. K. Gleason, *Chemistry of Materials* (available online).

72. http://electronics.howstuffworks.com/led1.htm

73. E. Holder, N. Tessler, and A. L. Rogach, *Journal of Materials Chemistry* 18, 1064 (2008).

74. V. L. Colvin, M. C. Schlamp, and A. P. Alivisatos, *Nature* 370, 354 (1994).

75. B. O. Dabbousi, M. G. Bawendi, O. Onitsuka, and M. F. Rubner, *Applied Physics Letters* 66, 1316 (1995).

76. M. C. Schlamp, X. G. Peng, and A. P. Alivisatos, *Journal of Applied Physics* 82, 5837 (1997).

77. H. Mattoussi, L. H. Radzilowski, B. O. Dabbousi, E. L. Thomas, M. G. Bawendi, and M. F. Rubner, *Journal of Applied Physics* 83, 7965 (1998).

78. S. Coe, W. K. Woo, M. Bawendi, and V. Bulovic, *Nature* 420, 800 (2002).

79. M. Y. Gao, B. Richter, and S. Kirstein, *Advanced Materials* 9, 802 (1997).

80. M. Y. Gao, C. Lesser, S. Kirstein, H. Mohwald, A. L. Rogach, and H. Weller, *Journal of Applied Physics* 87, 2297 (2000).

81. C. Y. Huang, Y. K. Su, T. S. Huang, Y. C. Cben, C. T. Wan, M. V. M. Rao, T. F. Guo, and T. C. Wen, *2008 Ieee Photonicsglobal@Singapore (Ipgc), Vols 1 and 2*, 258 (2008).

82. Y. Q. Li, A. Rizzo, M. Mazzeo, L. Carbone, L. Manna, R. Cingolani, and G. Gigli, *Journal of Applied Physics* 97 (2005).

83. S. Coe-Sullivan, W. K. Woo, J. S. Steckel, M. Bawendi, and V. Bulovic, *Organic Electronics* 4, 123 (2003).

84. C. W. Lee, C. H. Chou, J. H. Huang, C. S. Hsu, and T. P. Nguyen, *Materials Science and Engineering B-Solid State Materials for Advanced Technology* 147, 307 (2008).

85. P. O. Anikeeva, J. E. Halpert, M. G. Bawendi, and V. Bulovic, *Nano Letters* 7, 2196 (2007).

86. L. Kim, P. O. Anikeeva, S. A. Coe-Sullivan, J. S. Steckel, M. G. Bawendi, and V. Bulovic, *Nano Letters* 8, 4513 (2008).

Chapter Two

Conformal, Conducting Poly (3, 4-ethylenedioxythiophene) Thin Films Deposited Using Bromine as the Oxidant in a Completely Dry Oxidative Chemical Vapor Deposition Process (oCVD)

Hitesh Chelawat, Sreeram Vaddiraju and Karen Gleason, 'Conformal, Conducting Poly(3,4-ethylenedioxythiophene) Thin Films Deposited Using Bromine as the Oxidant in a Completely Dry Oxidative Chemical Vapor Deposition Process(oCVD)', ***Chemistry of Materials*** (available online).

ABSTRACT

Poly (3, 4-ethylenedioxythiophene) (PEDOT) thin films were obtained through oxidative chemical vapor deposition (oCVD) by using a new oxidant- bromine. The use of bromine eliminates any post processing rinsing step required with other oxidants like iron chloride and hence makes the process completely dry. Film properties are further compared with the PEDOT films deposited using iron chloride as the oxidant. Accelerated aging experiments shows longer retention of electrical conductivity for the PEDOT films obtained using bromine as the oxidant. Conductivities as high as 380 S/cm were obtained for PEDOT films deposited using bromine as the oxidant at 80 °C, which is significantly higher than that for PEDOT films deposited using iron chloride as the oxidant at the same temperature. Cross-sectional SEM of the PEDOT films deposited using bromine on silicon trench wafers demonstrates high conformal deposition of the films. All the results show the possibility of depositing highly conducting, conformal PEDOT films on any substrate including silicon, glass, paper and, plastic.

KEYWORDS: poly(3,4-ethylenedioxythiophene), oxidative chemical vapor deposition (oCVD), oxidant, iron chloride, bromine, conformal, conducting

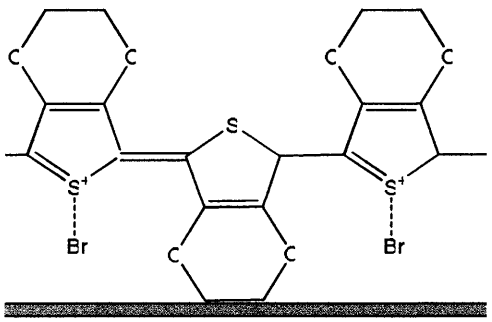

Figure 2-1: Poly (3, 4-ethylenedioxythiophene) deposited using bromine as the oxidant via oCVD process.

2.1 Introduction

Since their discovery in 1970[1], extensive research on conducting polymers has been motivated by potential applications for flexible electronic devices including light emitting diodes (LEDs), transistors, biosensors, biomedical devices, chemical sensors, solar cells, electrodes, microwave absorbing materials, new types of memory devices, nanoswitches, optical modulators and valves, imaging materials, polymer electronic interconnects, nanoelectronic and optical devices and nonlinear optical devices.[2-9] Conducting polymers show negligible conductivity in the neutral state. Conductivity results from the formation of charge carriers upon oxidation or reduction of their conjugated backbone.[10, 11] Difficulties with traditional methods of synthesis and film formation for conducting polymers, many of which are insoluble, motivate the development of alternate approaches, such as chemical vapor deposition (CVD).

The vapor deposition of both the oxidant and the monomer is termed the oxidative chemical vapor deposition (oCVD) method for growing conducting polymer thin films [12, 13]. Deposition of the poly (3,4-ethylenedioxythiophene) (PEDOT) films by oCVD using $FeCl_3$ has been described in detail in the literature[12]. With this method smooth PEDOT films with conductivities as >1000 S/cm has been obtained[13]. The compatibility of oCVD deposition of PEDOT has been demonstrated in the Fig. 2-2[14]. But one of the drawback of using iron chloride as the oxidant for the polymerization of EDOT is that it is not a completely dry process. Post processing of the oCVD PEDOT films deposited using iron chloride by methanol is required to remove the unreacted iron chloride, the reaction by-product $Fe(II)Cl_2$ and any oligomers or short chains formed during the polymerization process as they become contaminant during device fabrication.[12] In an attempt to make

the process completely dry, halogens are used as the replacement for iron chloride as the oxidant for the oCVD process in our experiments. Halogens have been widely used by the researchers as a dopant for making conducting polymers.[15-29] Mathai *et al.*[15] studied the effect of iodine doping on band gap of aniline thin films. Gal *et al.*[16] compared the electrical conductivity of poly (2-ethynylthiophene) and poly (2-ethynylfuran) doped with iodine, bromine and iron chloride. In most of the cases, doping of the polymers was done by dipping the polymer film in the bromine/iodine (or any other dopant) solution or by exposing to halogen vapor for sufficient time.

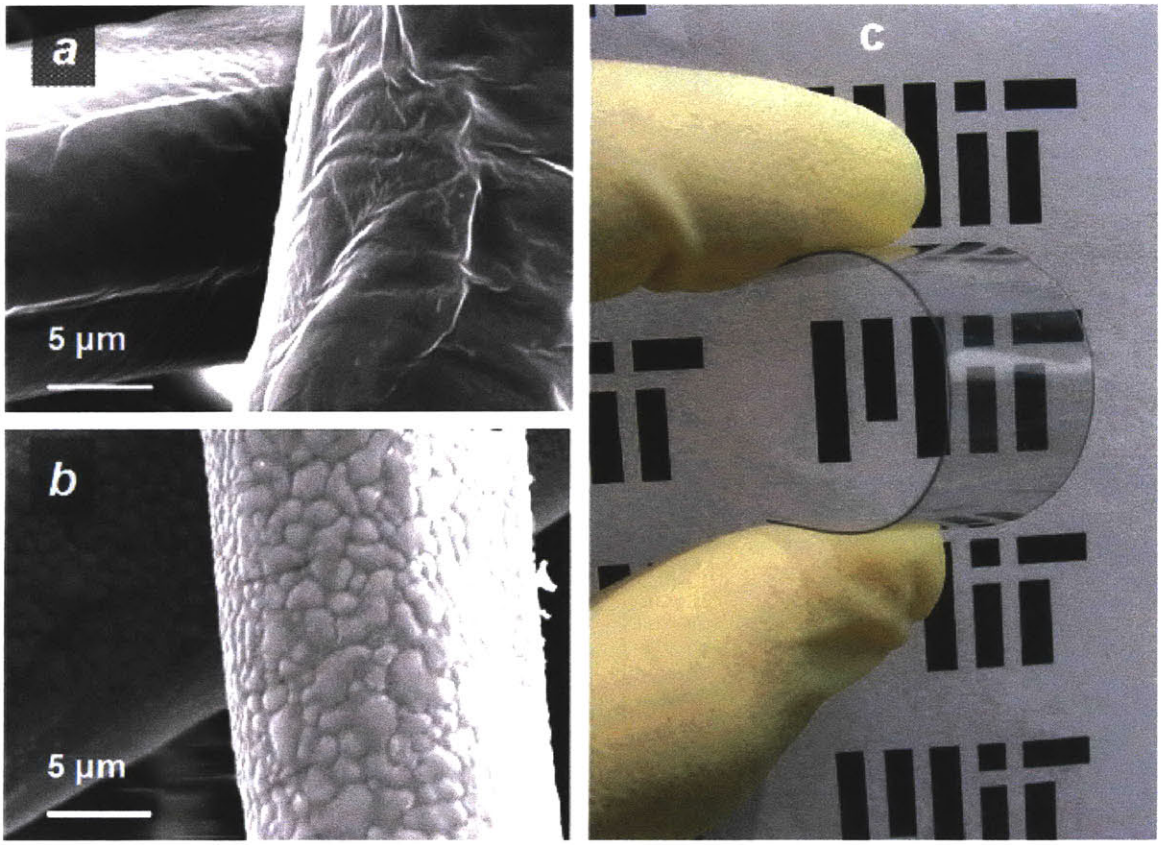

Figure 2-2: Compatibility of oCVD with various substrates is shown :- (a) SEM image of an uncoated paper towel fiber. (b) SEM image of a paper towel fiber coated with CVD PEDOT. (c) CVD PEDOT coating with 84% optical transmittance on flexible PET[14].

In the current work, a completely dry process utilizing bromine as the oxidant as well as the dopant is successfully demonstrated to deposit conductive PEDOT films with enhanced stability. In this paper, the notation Cl-PEDOT will refer to films deposited using iron chloride as the oxidant while Br-PEDOT will denote films deposited using bromine as the oxidant. Differences in the series of processing steps for the two oxidants are shown in Fig. 2-3. By avoiding the rinsing step we made it possible to deposit oCVD PEDOT film in a completely dry manner. A few of the advantages of making the process completely dry includes possibility of using solvent-sensitive substrates such as paper, overcoming the effects of rinsing on the underlying films in case of multilayer structure, avoiding exposure of the films to air while rinsing. In essence, it is now possible to carry out oCVD PEDOT deposition on any substrate in roll-to-roll or cluster tool processes.

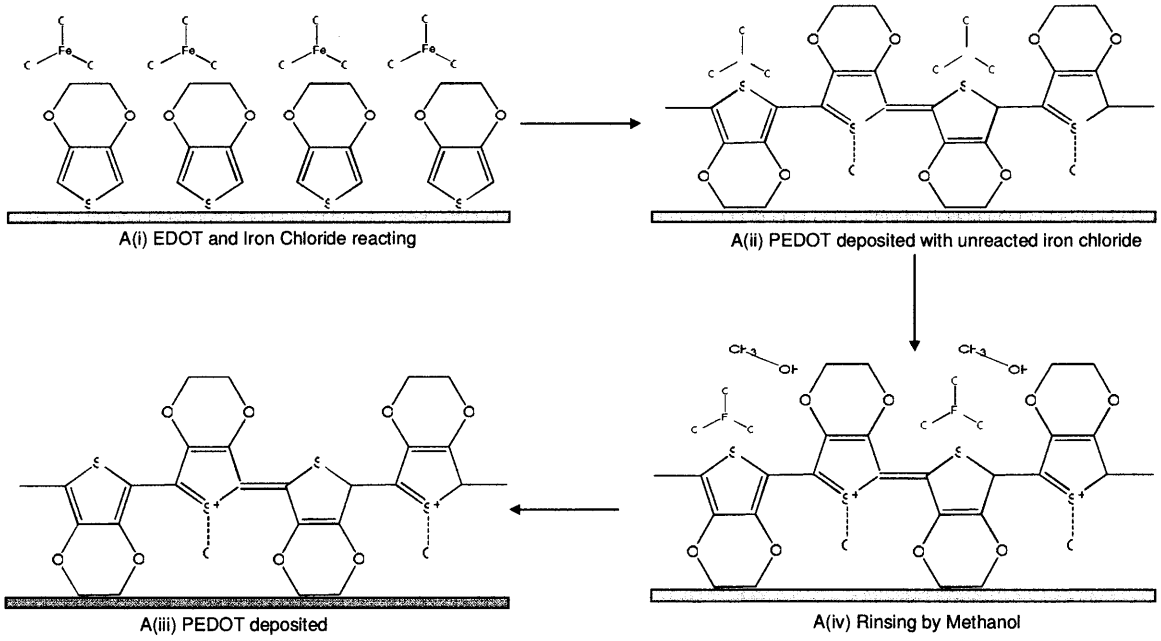

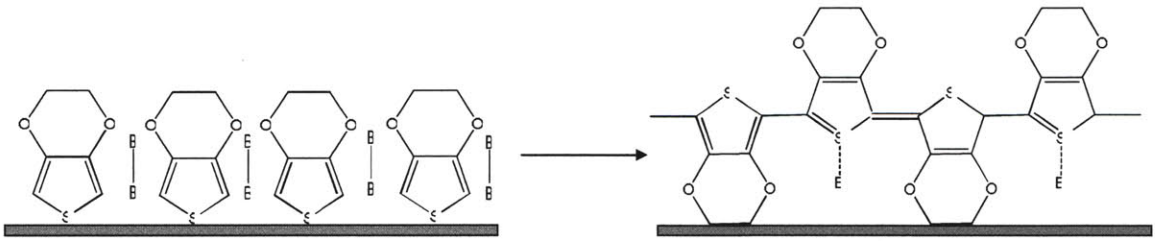

Figure 2-3: Steps in oCVD process of depositing PEDOT thin films using (A) Iron Chloride (B) Bromine as the oxidant. No post processing step was required in the case of bromine as the oxidant.

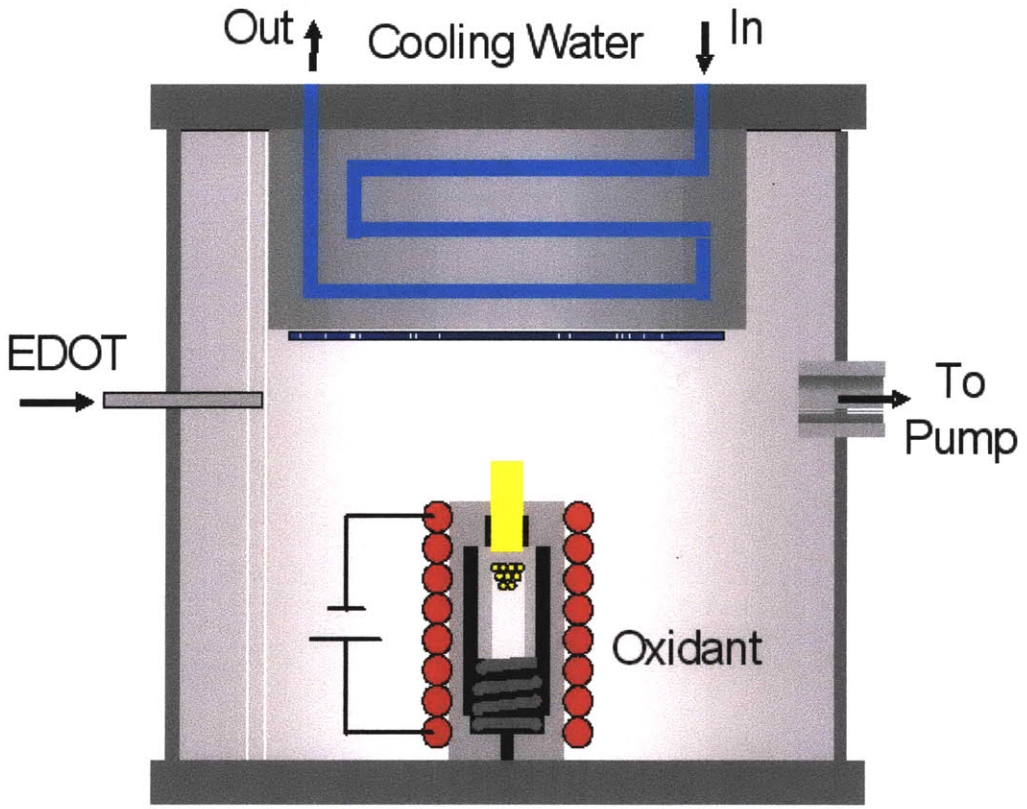

Figure 2-4: Schematic of an oCVD chamber

2.2 Experimental

Substrates used in the experiments were glass and silicon. Two different set of experiments were done using iron chloride ($Fe(III)Cl_3$) (97%, Aldrich) and bromine (Br_2) (reagent grade, Aldrich) as the oxidants. For the Cl-PEDOT films, iron chloride was thermally evaporated by resistive heating a crucible within the reaction chamber, as

previously described[12]. The schematic of the chamber is shown in the Fig. 2-4 above. For the Br-PEDOT films, bromine was delivered as a vapor through a side port of the same chamber. Since bromine is very volatile, no heating of the source jar or delivery lines was required. For both types of films, vapor phase EDOT monomer (3,4-ethylenedioxythiophene, Aldrich) as 3 sccm was delivered into the reactor from a side port. Source jar and feed lines were heated to 150 °C. The chamber pressure was maintained at 150 mtorr. All the chemicals were used as obtained from the vendors. Experiments were performed at a substrate temperature of 80°C so as to result in reasonably conducting films at reasonable deposition rates for both the oxidants. This temperature is not an optimized substrate temperature for either the bromine or the iron chloride doped PEDOT film deposition processes. The rest of the deposition process for Br-PEDOT remained similar to the oCVD process using iron chloride as the oxidant. Prior to each deposition, the reactor chamber was baked at 120 °C for several hours to reduce any contamination. Both films were grown to a total thickness of 40 nm. Deposition time for Cl-EPDOT films was 20 min. and for Br-PEDOT films was 40 min. Further details of the oCVD process and reaction chamber are published elsewhere.[12] After deposition, films deposited using iron chloride were rinsed with methanol where as films deposited using bromine were used as it is for characterization.

Fourier transform infrared(FTIR) measurements were performed on Nexus 870, Thermo Electron Corp. Composition of the films was estimated using x-ray photoelectron spectroscopy (XPS) (Surface Science Instruments (SSI) model SSX-100) utilizing monochromated Aluminum K-alpha x-rays (1486.6 eV) to strike a sample surface. Conformality studies and roughness studies were performed using scanning electron

microscope (SEM) (JEOL JSM- 6060) and atomic force microscope (AFM) (Digital Instruments, D 3100s-1). The thicknesses and conductivity of the films deposited on glass were measured using a KLA Tencor P-16 surface profilometer and with a four-point probe (Model Keithley SCS-4200), respectively. Conductivity values were calculated using the sheet resistivity measured by the four-point probe and thickness measured by the profilometer.

2.3 Results and Discussions

Characterization of the unrinsed (e.g. "all dry") Br-PEDOT and methanol-rinsed Cl-PEDOT films not only revealed several similarities between the films but also revealed several clear differences.

2.3.1 Chemical Bonding.

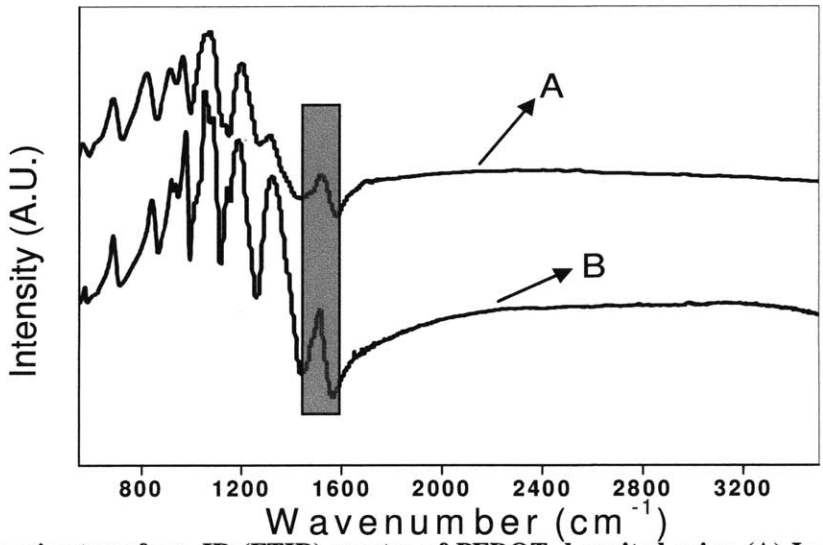

Figure 2-5: Fourier transform IR (FTIR) spectra of PEDOT deposited using (A) Iron Chloride (B) Bromine as the oxidant. Shaded rectangle highlights an absorption region associated with conjugation in oCVD PEDOT.

The similarity in the FTIR spectra of the Br-PEDOT and Cl-PEDOT (Fig. 2-5) clearly confirms the formation of doped PEDOT when using bromine as the oxidant. The

intensity of the C=C peak at 1520 cm^{-1} is higher for the Br-PEDOT than for the Cl-PEDOT. This increased intensity reflects a higher degree of conjugation, which in turn is expected to result in higher conductivity.[12,30-32]This result is in line with the observed conductivities of Br-PEDOT (380 ± 8 S/cm), and Cl-PEDOT (40 ± 1 S/cm). Conductivities of the oCVD PEDOT film obtained for this study were similar to those reported previously.[12]

Doping bands were observed at 1513, 1319, 1195, 1090, 1060, 980, 849 cm^{-1}, as expected for Cl-PEDOT.[33-35] The doping induced bands were observed to be shifted to lower wavenumbers in the Br-PEDOT film.[36] This shift to lower wavenumbers reflects the reduced bonding strength associated with substitution by the larger and heavier bromine atom (covalent radii of 0.1142 nm and ionic radii 0.196 nm versus a covalent radii of 0.099 nm and an ionic radii 0.181 nm for chlorine).[37]

2.3.2 Elemental Composition

The XPS survey scans of both Cl-PEDOT(Fig. 2-6a) and Br-PEDOT (Fig. 2-6b) films showed the presence of the characteristic elements C, O and S. The position of the C, O and S peaks in both the Cl-PEDOT and Br-PEDOT were identical and match well with the previous reports[38, 39]. For Cl-PEDOT, the high resolution scan for chlorine reveals a spin-split doublet Cl $2p_{1/2}$ and Cl $2p_{3/2}$ having a 1.6 eV energy splitting, as shown in the inset in Fig 2-6a. No bromine was detected in the Cl-PEDOT films.

For Br-PEDOT, the high resolution scan for bromine revealed a spin-split doublet Br $3d_{3/2}$ and Br $3d_{5/2}$ having a 0.9 eV energy splitting[40], as shown in inset in Fig 2-6b.

Additionally, a high resolution scan for chlorine in the Br-PEDOT film confirmed the absence of chlorine. This was done to ensure that there is no cross-contamination by chlorine in the Br-PEDOT films as both Br-PEDOT and Cl-PEDOT depositions were carried out in the same reactor. The absence of chlorine validates the hypothesis that bromine is the dopant species in Br-PEDOT. The ratio of Cl/S was 0.22 in the Cl-PEDOT films and for Br-PEDOT the ratio of Br/S was 0.21.

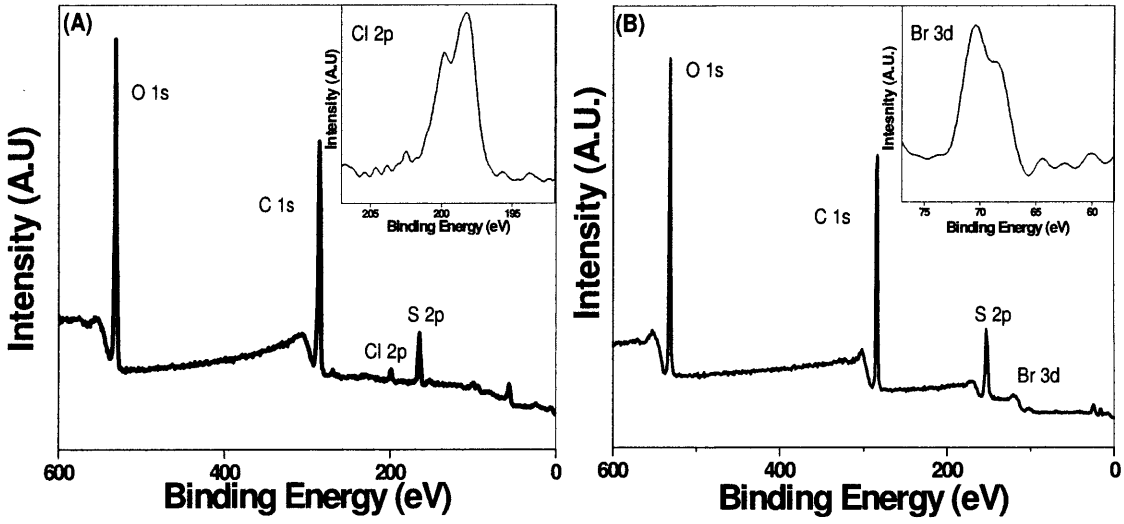

Figure 2-6: XPS survey scan of oCVD PEDOT deposited using (A) Iron Chloride (B) Bromine as the oxidant showing characteristic elements. Inset shows the high resolution scan for chlorine and bromine in Fig 2-6(A) and Fig 2-6(B) respectively.

2.3.3 Conformality

Electrical properties of the conducting polymers are strongly dependent on their film morphology and orientation of the chains.[41-44] Morphology of the oCVD films deposited using iron chloride has been studied before and very smooth films were obtained. Im *et al.* have used $CuCl_2$ as the oxidant for depositing PEDOT through oCVD but obtained

porous films because of weaker oxidizing strength of $CuCl_2$.[30] Bromine is a strong oxidizing agent, so smooth dense PEDOT films were anticipated. Indeed, oCVD PEDOT films deposited using bromine as the oxidant appeared smooth in SEM as shown in Fig. 2-7 a). AFM was conducted to compare the roughness of the films deposited using iron chloride and bromine as oxidants. Films deposited using iron chloride has roughness of ~5 nm whereas roughness of films deposited using bromine as the oxidant was ~ 4.5 nm slightly better than its counter part.

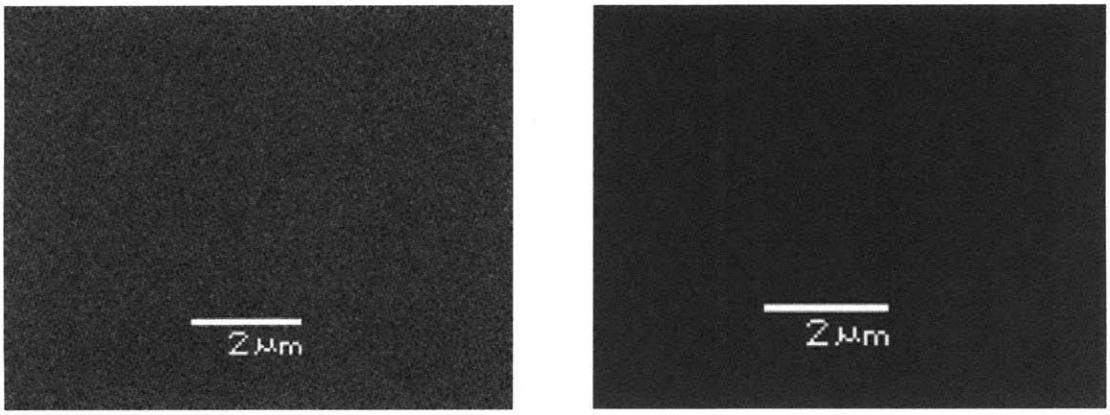

(A) (B)

Figure 2-7: SEM images of oCVD PEDOT deposited using (A) Iron Chloride (B) Bromine as the oxidant. AFM measurements give the roughness of PEDOT films in (B) as ~4.5 nm.

Trenches (8 µm deep X 2 µm wide) in silicon were used to examine the conformal coverage of oCVD PEDOT grown with bromine as the oxidant. Fig. 2-8 demonstrates the cross-sectional SEM image of the Br-PEDOT on the standard trenches. The cross-sectional image clearly shows the conformal deposition of the Br-PEDOT. Uniform deposition can be seen at both the side walls and the bottom of the trench. Conformal deposition is possible only in CVD process and very difficult to achieve in any other solution phase process. In the work previously done by our group[30], conformality studies

were done for PEDOT films deposited by spin casting and polymerizing a mixture of EDOT and $FeCl_3$ solution in methanol and were compared with oCVD PEDOT films grown with $CuCl_2$, $FeCl_3$ as the oxidants. In case of PEDOT films obtained by spin casting, solution was trapped at the bottom of the trench with depleted side walls and the top of the trench.

In case of oCVD PEDOT with $FeCl_3$, because of the directional deposition of $FeCl_3$ through the crucible, most of the deposition was on the entrance of the trench. Best conformality was reported for oCVD PEDOT films with $CuCl_2$ as the oxidant because of the volatility of Cl_2.[30] In case of Br-PEDOT also, high conformality was observed because of the volatility of Br_2 as compared to $FeCl_3$. We believe that high volatility of the oxidant improves the conformality because of very low sticking coefficient.

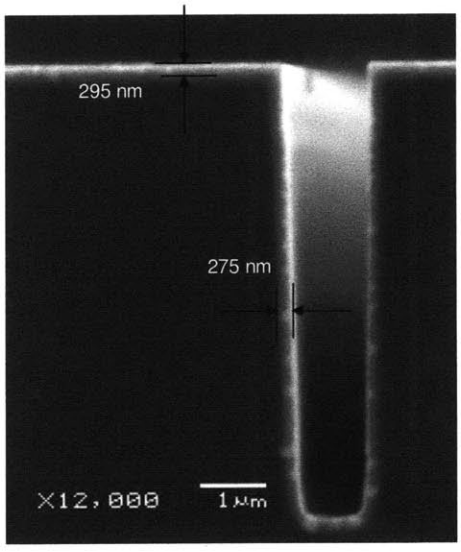

Figure 2-8 Cross-sectional SEM image of the oCVD PEDOT film deposited using bromine as the oxidant demonstrating high conformality of the deposition.

2.3.4 Conductivity

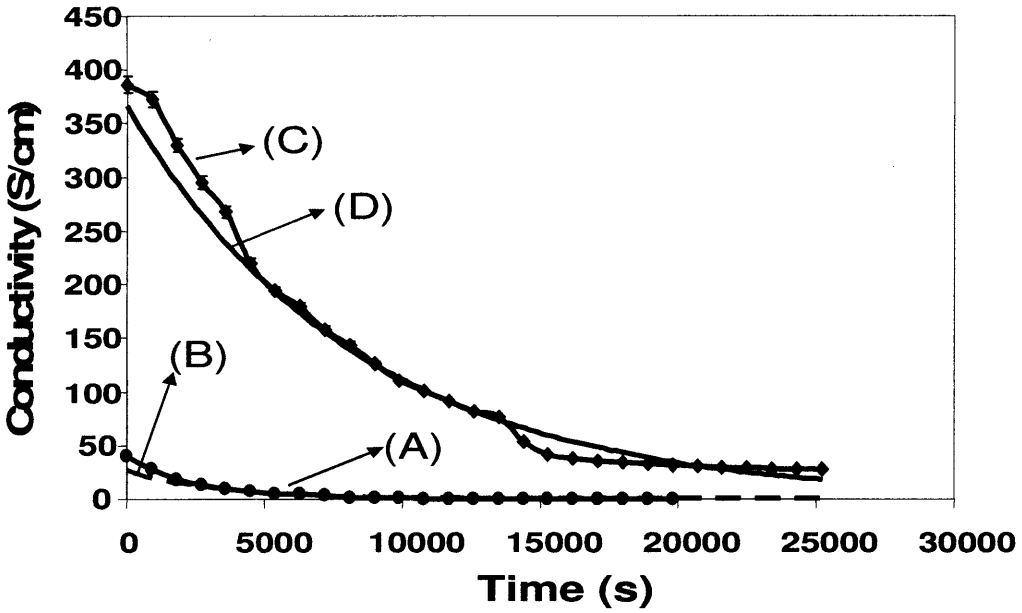

Figure 2-9 Show the results of accelerated aging experiments done on the oCVD PEDOT films at 100 °C. PEDOT Films were deposited using (A)Iron Chloride (C) Bromine as the oxidant. (B) and (D) are the exponential fits for (A) and (C) respectively.

Previously it has been shown that conductivity of the PEDOT films is a strong function of the conjugation length, dopant concentration and orientation of the PEDOT chains[12, 16, 38, 45]. Im *et al.*[12] showed that the substrate temperature affects the conjugation length of the deposited polymer therefore affecting the conductivity. In our experiments we measured conductivity for both the films deposited at 80 °C. oCVD PEDOT films deposited using bromine showed conductivity of ~380 ± 8 S/cm, an order of magnitude more than that of oCVD PEDOT films deposited using iron chloride (~40 ± 1 S/cm). The difference in conductivity in our experiments can be explained in terms of the difference in the conjugation length because of the higher oxidizing strength of bromine in comparison to the iron chloride[46] as also reflected in the FTIR data (Fig. 2-5).

Limited work has been reported on aging of PEDOT thin films.[47-51] On aging, the conductivity of the PEDOT film decreases because of the polymer chain oxidation and counter-ion degradation. Guiseppielie *et al.*[17] observed that iodine-doped polyacetylene films become less conducting over time because of the iodination of the polymer bone. It is believed that stability of PEDOT films can be increased by reducing the oxidation potential of the polymer chains. The conductivity of Br-PEDOT and Cl-PEDOT films in air at 100 °C reveal that films having bromine as a dopant are more stable (Fig. 2-9). Note this comparison is for films deposited at identical substrate temperature, as this parameter has often been correlated with the ultimate thermal stability of thin film. Note that the Br-PEDOT film had a higher value of initial conductivity, and it is unclear how, if at all, this property influences thermal stability. The conductivity of both types PEDOT films decayed exponentially with annealing time ($R^2 > 0.95$). The corresponding life times at 100 °C are 2,300± 115 s and 10,160 ± 510 s. The observed ~5-fold increase in the stability for the Br-PEDOT is significant for electronic device applications. Hence apart from making the process completely dry, more stable oCVD PEDOT films were deposited by using bromine as the oxidant.

2.4 Conclusions

Poly (3, 4-ethylenedioxythiophene)(PEDOT) thin films were obtained via oCVD process using bromine as the oxidant. Use of bromine resulted in a completely dry process with no post processing required. Br-PEDOT films when compared with Cl-PEDOT films show enhanced properties in terms of conductivity, conformality of the deposition and stability. Br-PEDOT films deposited at 80 °C showed conductivity of 380

± 8 S/cm where as Cl-PEDOT films showed conductivity of 40 ± 1 S/cm. Cross-sectional SEM image confirms the high conformality of the Br-PEDOT deposition. XPS study confirms that PEDOT films deposited using bromine have the identical characteristic peak positions for C, O, S as that of Cl-PEDOT. XPS also confirms that Br-PEDOT is conducting solely because of bromine as the dopant and not any other contamination. Br-PEDOT retains electrical stability longer during accelerated aging experiments in air because bromine is less volatile and has lower oxidation potential than chlorine. Enhanced stability will be critical in the application of PEDOT in device applications.

ACKNOWLEDGMENT. This work was supported by Eni S.p.A. under the Eni-MIT Alliance Solar Frontiers Program. We also thank Jonathan Shu from Cornell Center for Materials Research (CCMR) for his help with XPS measurements.

2.5 References

1. Heeger, A. J., Angewandte Chemie-International Edition 2001, 40, (14), 2591-2611.
2. Burroughes, J. H.; Bradley, D. D. C.; Brown, A. R.; Marks, R. N.; Mackay, K.; Friend, R. H.; Burns, P. L.; Holmes, A. B., Nature 1990, 347, (6293), 539-541.
3. Katz, H. E., Journal of Materials Chemistry 1997, 7, (3), 369-376.
4. Gerard, M.; Chaubey, A.; Malhotra, B. D., Biosensors & Bioelectronics 2002, 17, (5), 345-359.
5. Guimard, N. K.; Gomez, N.; Schmidt, C. E., Progress in Polymer Science 2007, 32, (8-9), 876-921.
6. Lange, U.; Roznyatouskaya, N. V.; Mirsky, V. M., Analytica Chimica Acta 2008, 614, (1), 1-26.
7. Angelopoulos, M., Ibm Journal of Research and Development 2001, 45, (1), 57-75.
8. Hoppe, H.; Sariciftci, N. S., Journal of Materials Research 2004, 19, (7), 1924-1945.
9. Moliton, A.; Hiorns, R. C., Polymer International 2004, 53, (10), 1397-1412.
10. Bredas, J. L.; Street, G. B., Accounts of Chemical Research 1985, 18, (10), 309-315.
11. Schueppel, R.; Schmidt, K.; Uhrich, C.; Schulze, K.; Wynands, D.; Bredas, J. L.; Brier, E.; Reinold, E.; Bu, H. B.; Baeuerle, P.; Maennig, B.; Pfeiffer, M.; Leo, K., Physical Review B 2008, 77, (8).
12. Im, S. G.; Gleason, K. K., Macromolecules 2007, 40, (18), 6552-6556.

13. Baxamusa, S. H.; Im, S. G.; Gleason, K. K., Physical Chemistry Chemical Physics 2009, 11, (26), 5227-5240.

14. Lock, J. P.; Im, S. G.; Gleason, K. K., Macromolecules 2006, 39, (16), 5326-5329.

15. Mathai, C. J.; Saravanan, S.; Anantharaman, M. R.; Venkitachalam, S.; Jayalekshmi, S., Journal of Physics D-Applied Physics 2002, 35, (17), 2206-2210.

16. Gal, Y. S.; Jung, B.; Choi, S. K., Journal of Applied Polymer Science 1991, 42, (6), 1793-1797.

17. Guiseppielie, A.; Wnek, G. E., Journal of the Chemical Society-Chemical Communications 1983, (2), 63-65.

18. Sinigersky, V.; Madec, P. J.; Marechal, E.; Schopov, I., Macromolecular Chemistry and Physics 1997, 198, (4), 919-925.

19. Touihri, S.; Bernede, J. C.; Molinie, P.; Legoff, D., Polymer 2002, 43, (10), 3123-3129.

20. Chiang, C. K., Physica a-Statistical Mechanics and Its Applications 2003, 321, (1-2), 139-151.

21. Ozaki, J.; Sunami, I.; Nishiyama, Y., Journal of Physical Chemistry 1990, 94, (9), 3839-3843.

22. Abbett, K. F.; Teja, A. S.; Kowalik, J.; Tolbert, L., Journal of Applied Polymer Science 2003, 90, (14), 3876-3881.

23. Alimi, K.; Ayachi, S.; Mabrouk, A.; Molinie, P.; Zaidi, B.; Bernede, J. C.; Ghedira, M., Journal of Applied Polymer Science 2002, 85, (9), 1858-1866.

24. Napo, K.; Safoula, G.; Bernede, J. C.; D'Almeida, K.; Touirhi, S.; Alimi, K.; Barreau, A., Polymer Degradation and Stability 1999, 66, (2), 257-262.

25. Svorcik, V.; Proskova, K.; Hnatowicz, V.; Rybka, V., Nuclear Instruments & Methods in Physics Research Section B-Beam Interactions with Materials and Atoms 1999, 149, (3), 312-318.

26. Komarudin, D.; Morita, A.; Osakada, K.; Yamamoto, T., Polymer Journal 1998, 30, (10), 860-862.

27. Louboutin, J. P.; Beniere, F., Journal of Physics and Chemistry of Solids 1982, 43, (3), 233-241.

28. Wang, L. X.; Jing, X. B.; Wang, F. S., Synthetic Metals 1991, 41, (1-2), 739-744.

29. Tashiro, K.; Kobayashi, M.; Kawai, T.; Yoshino, K., Polymer 1997, 38, (12), 2867-2879.

30. Im, S. G.; Kusters, D.; Choi, W.; Baxamusa, S. H.; de Sanden, M.; Gleason, K. K., Acs Nano 2008, 2, (9), 1959-1967.

31. Tran-Van, F.; Garreau, S.; Louarn, G.; Froyer, G.; Chevrot, C., Journal of Materials Chemistry 2001, 11, (5), 1378-1382.

32. Chiu, W. W.; Travas-Sejdic, J.; Cooney, R. P.; Bowmaker, G. A., Synthetic Metals 2005, 155, (1), 80-88.

33. Kvarnstrom, C.; Neugebauer, H.; Blomquist, S.; Ahonen, H. J.; Kankare, J.; Ivaska, A.,Electrochimica Acta 1999, 44, (16), 2739-2750.

34. Kvarnstrom, C.; Neugebauer, H.; Blomquist, S.; Ahonen, H. J.; Kankare, J.; Ivaska, A.; Sariciftci, N. S., Synthetic Metals 1999, 101, (1-3), 66-66.

35. Winther-Jensen, B.; West, K., Macromolecules 2004, 37, (12), 4538-4543.

36. Thomas, K. R. J.; Lin, J. T.; Hsu, Y. C.; Ho, K. C.,Chemical Communications 2005, (32), 4098-4100.

37. Chen, G. H.; Gupta, M.; Chan, K.; Gleason, K. K., Macromolecular Rapid Communications 2007, 28, (23), 2205-2209.

38. Im, S. G.; Olivetti, E. A.; Gleason, K. K., Surface & Coatings Technology 2007, 201, (22-23), 9406-9412.

39. Im, S. G.; Yoo, P. J.; Hammond, P. T.; Gleason, K. K., Advanced Materials 2007, 19, (19), 2863.

40. Basu, R.; Kinser, C. R.; Tovar, J. D.; Hersam, M. C., Chemical Physics 2006, 326, (1), 144-150.

41. de Jong, M. P.; van Ijzendoorn, L. J.; de Voigt, M. J. A., Applied Physics Letters 2000, 77, (14), 2255-2257.

42. Makinen, A. J.; Hill, I. G.; Shashidhar, R.; Nikolov, N.; Kafafi, Z. H., Applied Physics Letters 2001, 79, (5), 557-559.

43. Pacios, R.; Bradley, D. D. C., Synthetic Metals 2002, 127, (1-3), 261-265.

44. Cao, Y.; Yu, G.; Zhang, C.; Menon, R.; Heeger, A. J., Synthetic Metals 1997, 87, (2), 171-174.

45. Baik, W.; Luan, W. Q.; Zhao, R. H.; Koo, S.; Kim, K. S., Synthetic Metals 2009, 159, (13), 1244-1246.

46. Vaddiraju, S.; Senecal, K.; Gleason, K. K., Advanced Functional Materials 2008, 18, (13), 1929-1938.

47. Huang, J.; Miller, P. F.; de Mello, J. C.; de Mello, A. J.; Bradley, D. D. C., Synthetic Metals 2003, 139, (3), 569-572.

48. Heywang, G.; Jonas, F., Advanced Materials 1992, 4, (2), 116-118.

49. Winter, I.; Reese, C.; Hormes, J.; Heywang, G.; Jonas, F., Chemical Physics 1995, 194, (1), 207-213.

50. Rannou, P.; Nechtschein, M., Synthetic Metals 1999, 101, (1-3), 474-474.

51. Pei, Q. B.; Zuccarello, G.; Ahlskog, M.; Inganas, O., Polymer 1994, 35, (7), 1347-1351.

Chapter Three

Development of Hybrid Light Emitting Diodes Using Conducting Polymers Deposited by oCVD Process

ABSTRACT

For organic-light emitting diode (OLED) technology, optimization of production such that it is simple and scalable is necessary to compete with traditional incandescent and fluorescent light sources. In this work, we report a technology to make efficient, cheap and stable hybrid light emitting diodes (HLED) with roll-to-roll processing. Organic materials such as polyphenylenevinylene (PPV), currently employed in most of the OLED and HLED easily oxidize in air so require packaging layers and ultrahigh vacuum tools for fabrication. In our method, all the materials used in fabricating the device are stable in air and after the deposition of electrode bilayer, the remaining fabrication is done in air. The configuration of the device fabricated is ITO/ poly (EDOT-co-TAA)/ CdSe (ZnS)/Au. Oxidative chemical vapor deposition process is used to deposit poly (EDOT-co-TAA). CdSe (ZnS) is further attached to the ITO/poly (EDOT-co-TAA) surface using a linker molecule. Covalent interfacing results in enhanced charge transfer, low operating voltages and robust design. A photoluminescence spectrum indicates coalescence-free assembly of CdSe (ZnS) quantum dots with full width half maxima of 33 nm. Operating voltages as low as 4.3 V have been obtained so far and with further optimization of the device layers, we expect it to drop below 4 V. Preliminary results look promising for the development of air-stable and efficient HLED.

3.1 Introduction

Inorganic LEDs are widely used today. Robust blue, green, and red light emitting diodes are available in the market but separate structures, materials, and growth processes are required to achieve the different colors, thus resulting in completely different devices. For making blue and green light emitting diodes, alloys of InGaAlN are used with each color requiring a uniquely different alloy composition. Red LEDs are primarily made of InGaAsP which is a different compound altogether. On the other hand, organic LEDs (OLEDs) offer the advantage of color change from blue to red or orange by simply adding dyes in minute amounts to the optically active organic electroluminescent layer. Alternatively organic materials are coated on OLED to convert the light emitted to longer wavelengths (color converters). However, limitations of OLEDs as the underlying light source include problems with degradation of diode performance during electrical operation and the unavailability of efficient blue emitting materials. An additional problem is that of the sensitivity of organic OLEDs to subsequent processing in that they cannot be subjected to temperatures above, typically, 100° C and cannot be exposed to solvents such as water [1, 2]. These limitations call for more robust OLEDs.

One way to overcome these issues is to fabricate hybrid light emitting diodes (HLED) which incorporate the best qualities of both organic and inorganic LED. Most exciting and promising of HLED's are the ones based on quantum dots. Application of quantum dots (QDs) in HLED offers various advantages including high chemical and optical stabilities, easy tuning of the saturated color emission across the visible-NIR range, and easy processability in hybridizing organic and inorganic materials. QDs based HLED reported in literature uses organic material like PPV[3] or metal electrode like

Mg/Ca[4-6]. Operating lifetimes of devices based on PPVs are sensitive to its exposure to air. Xing et al. reported the oxidation behavior of PPV which results in black spot formation and loss of luminescence. Application of forward bias was found to accelerate the oxidation behavior[7]. When an organic light emitting diode is operated under ambient atmosphere, dark spot formation leads to complete device degradation within a few hours. Degradation of OLEDs on exposure to air and water vapor has been attributed to various mechanisms, including crystallization of the organic solids[8, 9], electrochemical reactions at the electrode/organic interface[10], migration of ionic species[11], and electrochemical reactions[12]. Cathode oxidation and cathode delamination were proven to be largely responsible for the growth of non-emissive spots on the emitting device area[13, 14]. Schaer et al. studied water vapor and oxygen degradation mechanisms in OLEDs[15]. Water vapor led to faster dark spot growth by almost three orders of magnitude than the evolution of dark spots under oxygen. Defect sites, such as pinholes appeared to be the degradation sites in both the cases leading to black spot formation as shown in the Fig. 3-1.

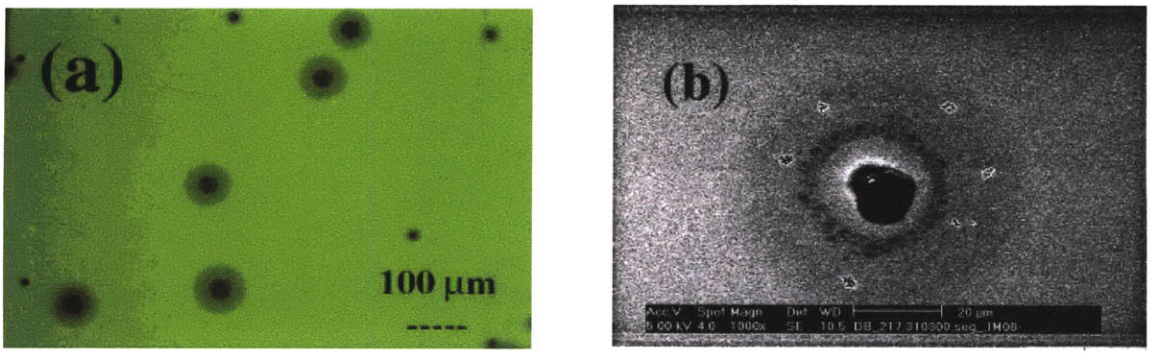

Figure 3-1: a) Optical microscopy image of an OLED working under a pure oxygen atmosphere showing dark spots. b) SEM image showing the formation of black spot on the aluminum cathode surface under operation in a pure oxygen atmosphere.

A technology developed in our lab to manufacture stable, efficient, and cheap hybrid light emitting diodes is being reported. The device can be configured as ITO/poly

(EDOT-co-TAA)/CdSe (ZnS)/Au. After the deposition of the electrode bilayer, the remaining fabrication is done in air and there is no need for an expensive cluster tool to transfer the device between fabrication steps under vacuum. Quantum dot (QD) attachment is done through a linker molecule. Photoluminescence spectrum has shown no coalescence of QDs on the substrate after deposition. The best operating voltages for the device so far obtained is as low as 4.3 V without any optimization of different layers in the device. With further optimization of different layers, we expect operating voltages to drop below 4V.

3.2 Experimental

Substrates used in these experiments were ITO coated glass obtained from Delta Technologies Ltd. (R_{sheet} ~ 5-15 Ω/□). ITO was etched out using 50:50 H_2O_2 (50 wt% in water solution):H_2SO_4 (95.0 -98.0 %) solution to obtain three 3 mm wide ITO line at 6 mm spacing. The substrates were cleaned by detergent, DI water, and isopropyl alcohol sequentially. They were then dried by blowing pressurized air and kept under vacuum. Just before device fabrication, further cleaning was done by oxygen plasma for 20 minutes. After oxygen plasma treatment, samples were dipped in thiophene-3-acetic acid (TAA) solution in methanol for 30 minutes to allow chemisorption of TAA on the substrate. This was done to improve the adhesion of poly (3, 4-ethylene dioxythiophene-co-thiophene-3-acetic acid) film on the substrate. Synthesis of poly (3, 4-ethylene dioxythiophene-co-thiophene-3-acetic acid) film was done using the oCVD approach. The reactor employed for this purpose is described in previous chapter. The reactor consists of a crucible filled with oxidizing agent, placed directly below the substrate in a

vacuum chamber. The substrate was held facing down towards the crucible containing the oxidizing agents. The temperature of the substrate and the crucible heater were capable of being heated independently and controlled by feedback. The pressure inside the chamber was controlled using a feedback controlled pressure valve, coupled with a mechanical pump. Iron chloride ($FeCl_3$) was employed as the oxidizing agent in all the experiments in this chapter. All the experiments were performed at low pressures ~150 mtorr. Substrate temperature was maintained at 80 ^{0}C whereas TAA and EDOT were heated to 180 ^{0}C and 150 ^{0}C respectively. Both EDOT and TAA were passed for about 20 minutes while maintaining the pressure of 100 mtorr above the base pressure. After the deposition of poly (EDOT-co-TAA), samples were rinsed with methanol to get rid of excess iron chloride. This poly (EDOT-co-TAA) acts as the hole-transport layer (HTL) in the device. Similar layers of homopolymer poly (3, 4-ethylenedioxythiophene) were used as a control HTL. After this deposition, substrate was dipped in a 0.01 M N,N'-dicyclohexylcarbodiimide (DCC) and 0.01M N-hydroxysuccinimide (NHS) solution in 50:50 molar ratio. DCC acts as catalyst to activate the -COOH group on the substrate. After 5 minutes, 0.01 M p-phenylenediamine (PDA) solution was added into the solution for 2 hrs. Substrate was then taken out of PDA solution and is dipped into QD solution and 1 ml each of 0.001 M NHS and 0.001 M DCC solution was added to activate the mercaptoudecanoic acid attached to the QDs. QD solution was prepared by taking 1 ml of QD (water soluble CdSe (ZnS) QDs obtained from NN labs) and diluting it with 50 ml of distilled water and ultrasonicating it for 1 hour. Activated -COOH functional group of mercaptoudecanoic acid (ligand attached to QDs) attaches itself to the amine group in the PDA on the substrate in 2 hours. Substrate was then taken out of the solution and rinsed

with methanol to get rid of any impurities and non-covalently bonded chemicals lying on it. After rinsing with methanol, a mask was placed on the substrate and a 40 nm gold layer which acts as cathode was deposited through sputtering. To make good electrical contacts, silver paste was deposited on the ITO and Au. Silver paste was prepared by mixing colloidal silver liquid and fast drying silver paint obtained from Electron Microscopy Sciences and Ted Pella, Inc., respectively. Final device structure is shown in the Fig. 3-2.

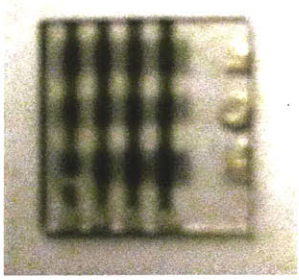

Figure 3-2: Digital image of the device fabricated.

Fourier transform infrared (FTIR) measurements were performed on Nexus 870, Thermo Electron Corp. Conformality studies and roughness studies were performed using scanning electron microscope (SEM) (JEOL JSM- 6060). The IV curves for the devices were measured on Keithley SCS-4200). In Photoluminescence measurements, samples were excited with a coherent Ti-Sapphire laser with a wavelength of 390 nm, a pulse width of 160fs, and a repetition rate of 250 kHz. A PI Acton SpectraPro SP-2360 Imaging Spectrograph with a PIXIS: 400B Digital CCD camera system was used to collect emitted photons. All measurements were carried out at room temperature.

3.3 Results and Discussions

The energy alignment of the ground and excited electronic states of QD monolayer and the surrounding organic thin films in a QD-LED plays an important role

in the operation of LED. HOMO level for the hole-transporting material is typically positioned between 5.0 and 6.0 eV below the vacuum level. So, there is a significant potential energy step for the hole injection into the QD valence band positioned >6 eV below the vacuum level[16]. And since the LUMO bands of organic electron-transporting materials are usually between 2.0 and 3.5 eV below the vacuum level[17], no potential barrier exists for electron injection into the QD conduction bands that are usually between 4.0 and 4.8 eV below the vacuum level[16]. Though the insulating layer of organic ligands that are passivating the QD surface act as a barrier for electron injection but in practicality, the ligand layer is typically $\leq$0.5 nm thick, so it forms a minimal tunneling barrier for the carriers that pass through it.

The difference in potential barriers for hole and electron injection into QDs results in carrier imbalance at QD sites and formation of electron-exciton pairs that recombine via the Auger mechanism[18]. As the organic hole-transporting materials with low HOMO level are not readily available, QD-LED performance can be improved by developing hole-transporting layer with HOMO level that can be tuned accordingly. Im et al. has shown the possibility of tuning work function of PEDOT by varying the reaction parameters[19]. Tuning of the work function of poly(EDOT-co-TAA) used as hole-transporting would be useful in optimizing the functioning of the device.

The configuration of the device fabricated can be depicted as ITO/ poly (EDOT-co-TAA)/ CdSe (ZnS)/ Au as shown in the Fig. 3-3:-

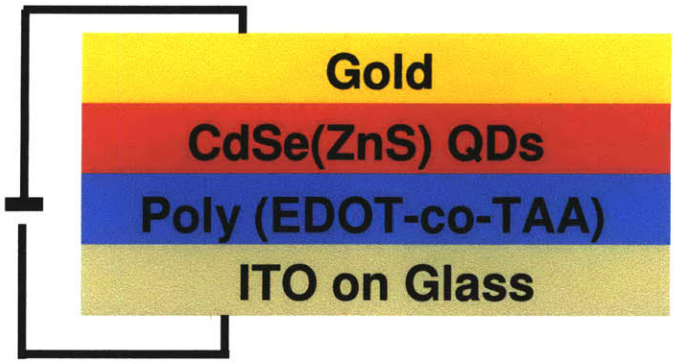

Figure 3-3: CdSe (ZnS) based QD-HLED design

The energy diagram and chemical structures of the various compounds used in the fabrication of the device are shown below in the Fig. 3-4 and Fig. 3-5, respectively.

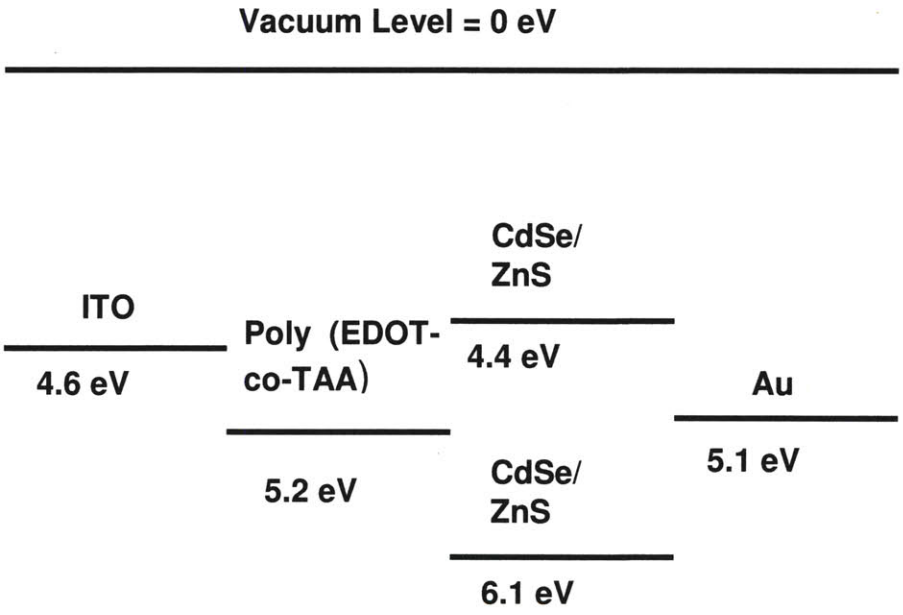

Figure 3-4: Energy levels of CdSe (ZnS) QD in the HLED design.

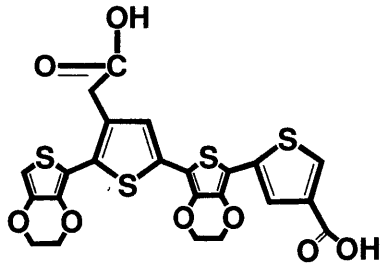

Poly (EDOT-co-TAA)

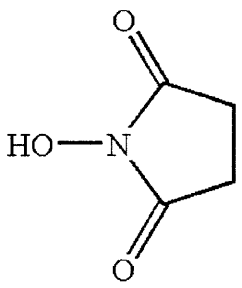

***N*-Hydroxysuccinimide (NHS)**

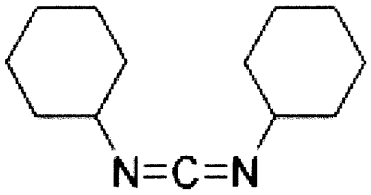

***N,N'*-Dicyclohexylcarbodiimide (DCC)**

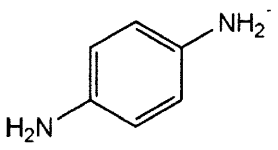

P-phenylenediamine (PDA)

Figure 3-5: Chemical structure of the compounds used in HLED fabrication.

Covalent interfacing results in enhanced charge transfer, low operating voltages and robust design. This device structure is very similar to the one reported by Colvin et al. in the first paper on hybrid LEDs[20]. Hexane dithiol was used to bind QDs to the hole-transport layer PPV. But unlike PPV, poly (PEDOT-co-TAA) used in our device is stable in air. Also the linker molecule used was aliphatic in nature, whereas we are using an aromatic linker molecule which enhances the charge transfer between HTL and QDs because of conjugation .Overall, using covalent bonding reduces the barrier for charge injection at the interface from hole-transport layer and electron transport layer to QDs. This results in low operating voltages. It also overcomes the limitations put by spin-casting of QDs on the substrate. Spin-casting of QDs is done either alone[6] or in blend with a polymer[21]. Spin-casting uses a solvent like toluene which puts restriction on the organic materials that can be used in device fabrication.

The various device layers were chemically, optically, and electronically characterized as described in the following section: -

3.3.1 Chemical Bonding

As shown in the previous chapter, we have been successfully depositing PEDOT using both bromine and iron chloride as oxidant in the oCVD reactor. Below is the FTIR for PEDOT deposited using iron chloride (Fig. 3-6(a)). Presence of 1520 cm^{-1} peak shows the conjugation in the system and its intensity shows the degree of conjugation. The peaks at 1090cm^{-1} and 1060 cm^{-1} corresponds to the stretching vibrations of bridged C-O in the ethylenedioxy group of EDOT and the band at 920cm^{-1} is the ethylenedioxy ring deformation mode[22].

Previously in our group, researchers had successfully deposited –COOH functionalized conducting copolymer films of Poly (pyrrole-co-thiophene-3-acetic acid) and used it for assembly of inorganic nanoparticles[23]. Variation in the gas phase feed ratio of pyrrole to TAA was used to vary the composition of the copolymer film. This allows tuning of conductivity and –COOH functionality of the copolymer films. The formation of PTAA was confirmed by the presence of carbonyl (-C=O) peak at 1721 cm^{-1}, C-H (2874, 2925, 2980 cm^{-1}) from the aliphatic $-CH_2$ group and aromatic C-H's of TAA, and -OH vibration mode from the acid group at 3460 cm^{-1} in the FTIR of the film shown in Fig. 3-6(b)[23, 24]. No peak was present at 685 cm^{-1} which represents α-β defects in the PTAA polymer[25].

Fig. 3-6(c) shows the FT-IR spectrum of oCVD grown poly (EDOT-co-TAA) film. The presence of C=O (1716cm^{-1}) from –COOH group and C-H (2874, 2925, 2984

cm^{-1}) from the aliphatic $-CH_2$ group and aromatic C-H's of TAA along with all the peaks of EDOT, as mentioned above, proved the presence of TAA in the copolymer. Retention of the characteristic peaks of TAA even after rinsing the polymeric films with methanol proved that the monomers reacted with each other and the film was not a simple mixture of either monomer.

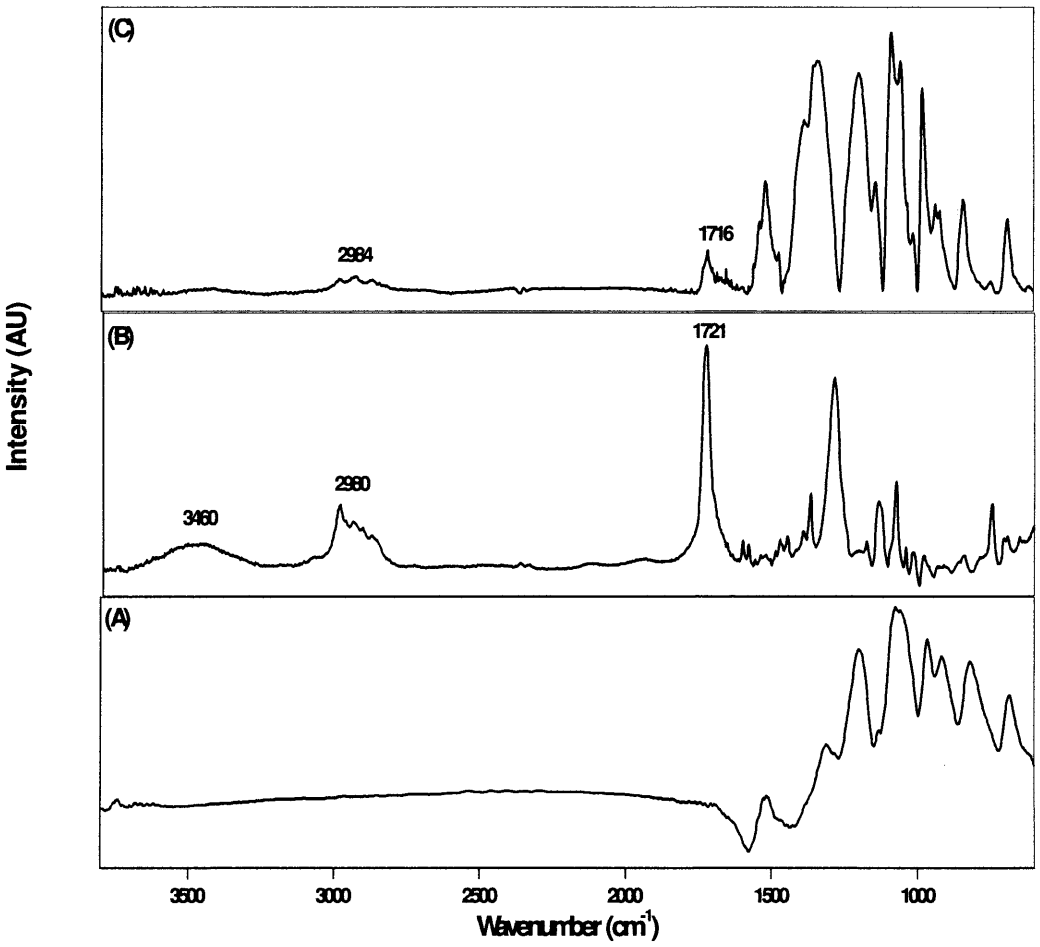

Figure 3-6 Fourier transform-IR (FTIR) spectra of (A) PEDOT (B) PTAA (C) Poly (EDOT-co-TAA) deposited using iron chloride as the oxidant.

3.2 Assembly of Quantum dots

Red and green CdSe (ZnS) quantum dots were covalently attached to the ITO/Poly (EDOT-co-TAA) using a diamine linker molecule (p-phenylenediamine). Uniform coalescence-free assembly of quantum dots was obtained as shown in the Fig. 3-7. SEM image (Fig. 3-8) of the sample also confirms uniform deposition of the QDs.

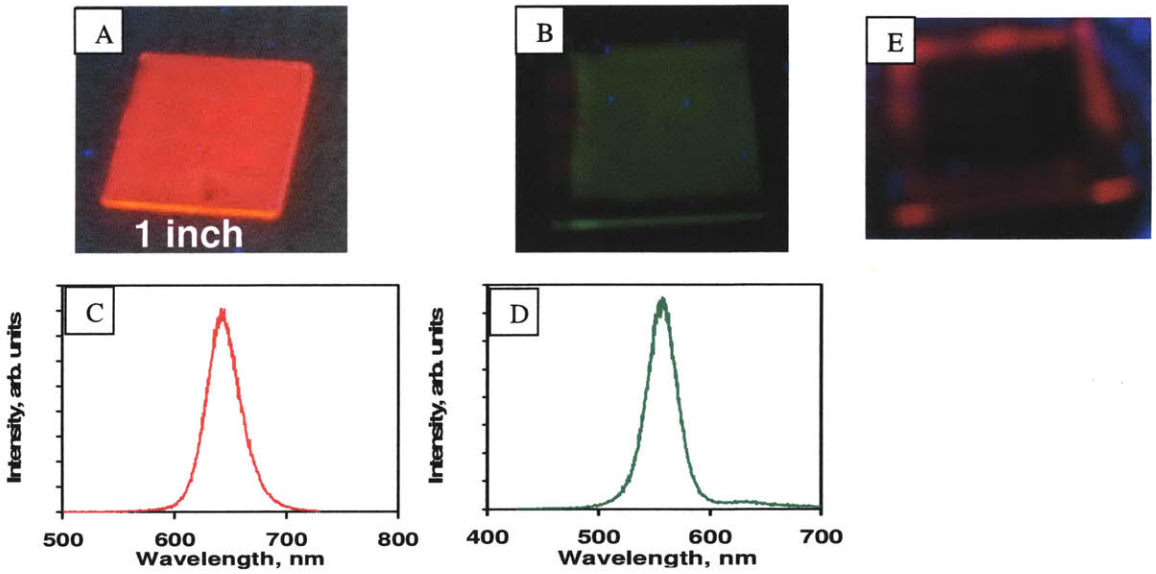

Figure 3-7 A) and B) show emission from uniform assembly of red and green QD LED under laser. C) and D) shows photoluminescence spectra having a sharp peak with FWHM of ~ 30 nm. (Courtesy: Sreeram Vaddiraju). E) Shows no adhesion of QDs on the PEDOT layer (in the center) used as HTL in the control device.

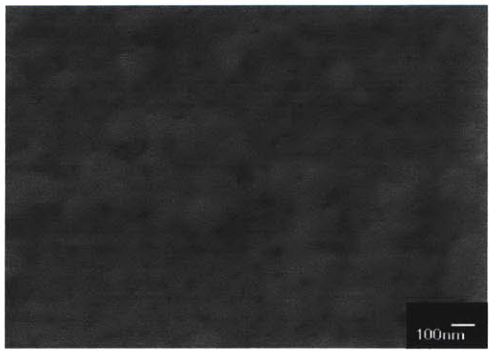

Figure 3-8: SEM image of uniform assembly of red QDs on the substrate (Courtesy: Sreeram Vaddiraju).

3.3 IV curves

3.3.1 Red Light Emitting Diodes

Sputtering of gold target was done to deposit the cathode. Control devices were prepared by depositing homopolymers poly (3, 4-ethylenedioxythiophene) as HTL. Device showed ohmic behavior with very low resistance as shown in the Fig. 3-9 below. The straight horizontal line in the IV curve implies that the current reached the saturation limit set at 0.01 A in the instrument.

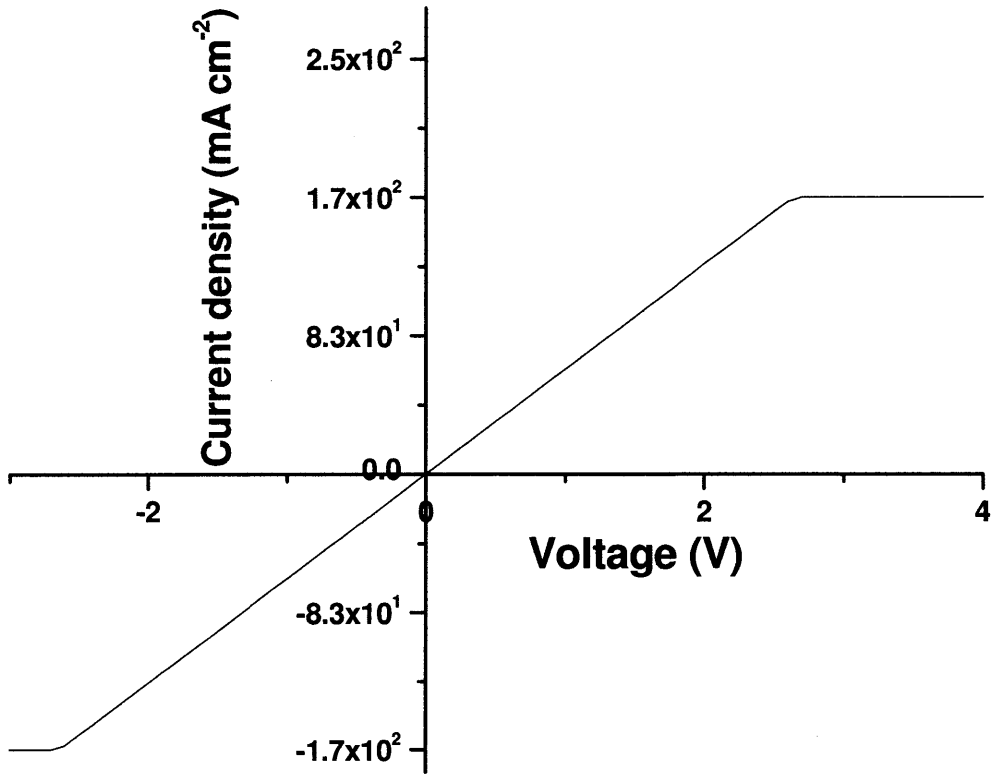

Figure 3-9 I-V characteristics of an unsuccessful control device prepared using PEDOT as HTL.

Some of the test devices did not display diode IV characteristics as shown in the Fig. 3-10 below. A possible reason for failure of some devices is poor adhesion of QDs in

some places on the substrate because of non-uniformity or lack of –COOH functional groups in the poly (EDOT-co-PTAA) films deposited on the substrate.

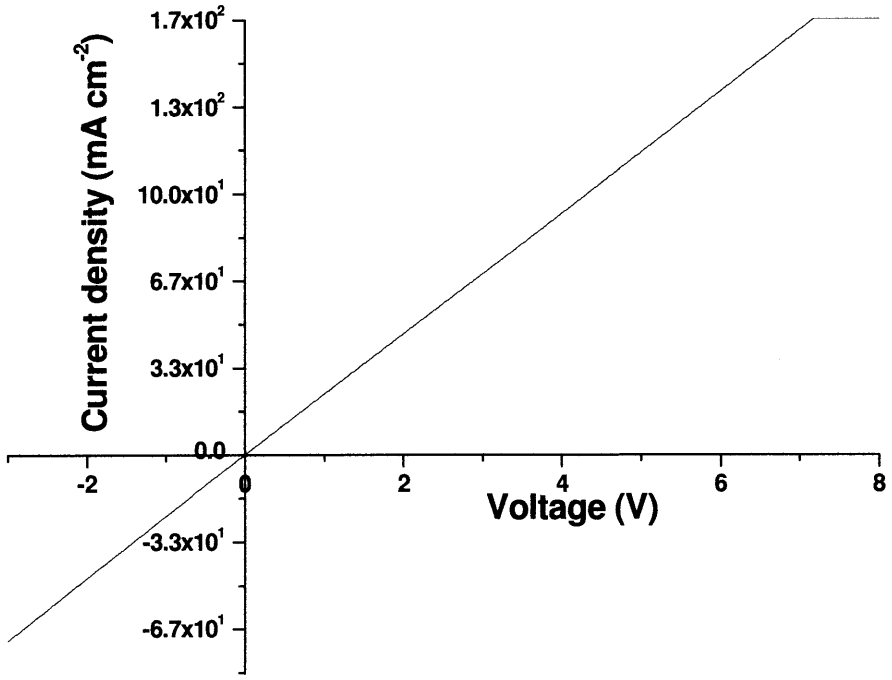

Figure 3-10: I-V characteristics of an unsuccessful device showing ohmic behavior.

Some of the devices displayed IV characteristics (Fig. 3-11), but no light emission was seen upon application of forward bias. Also at very low forward bias, significant current was passing in the device because of the high leakage current in the device. The lack of light emission may indicate the presence of recombination centers occurring from poor interfaces and presence of defects within the layers. This is also consistent with the very low current density measured.

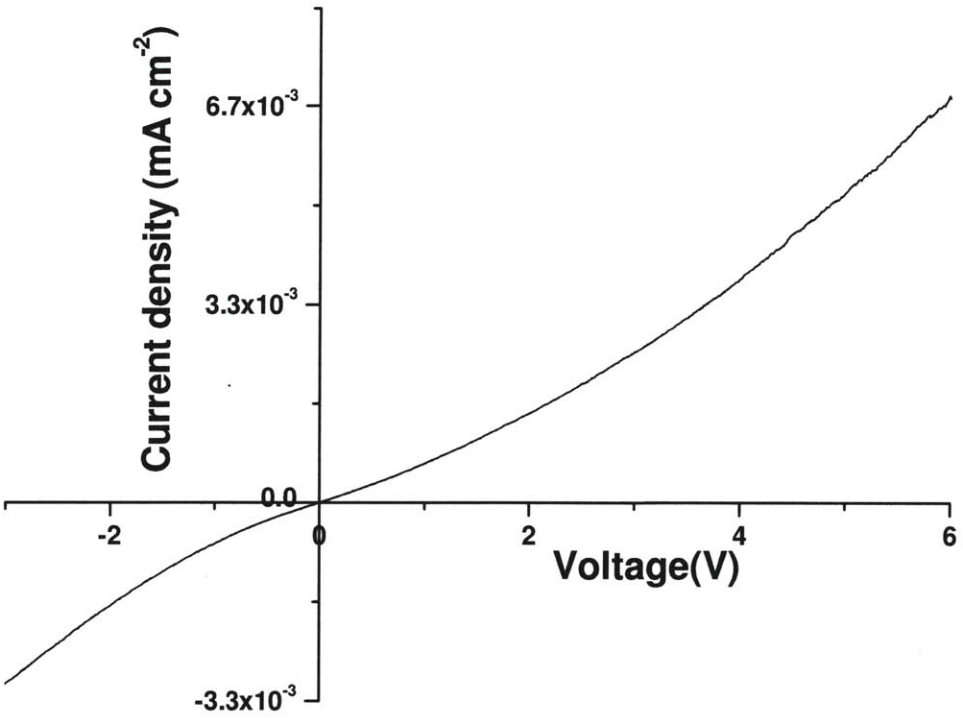

Figure 3-11: I-V characteristics of the device showing diode behavior. This device was not emitting light.

Several devices displayed desirable IV curves and also emitted red light on application of forward bias as shown in the Fig. 3.12: -

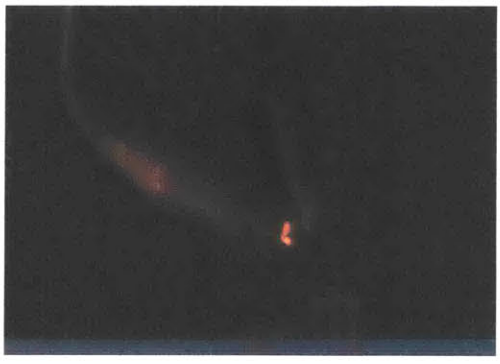

Figure 3.12: A picture showing working red LED.

The IV curve for a working device is shown in the Fig. 3-13. The operating voltages for the device were very different though the only parameter changing was the thickness and TAA content of poly (EDOT-co-TAA) layer, suggesting the importance of

this layer. Systematic conclusions would require an improvement in yield and reproducibility of the fabrication procedure. The operating voltage for the device displayed in Fig. 3-13 was 4.3 V even though there was significant leakage current. The straight horizontal line starting from 4V is because of the device reaching saturation limit for the current set at 0.01 A in the instrument.

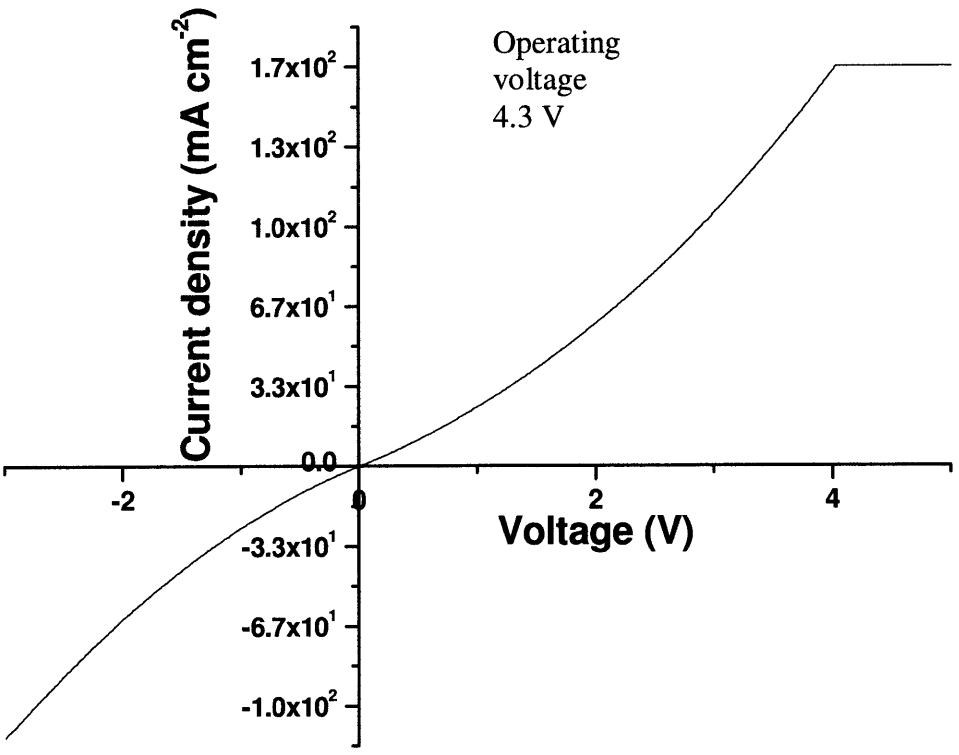

Figure 3-13: I-V characteristics of a working LED with operational voltage of 4.3 V.

Fig. 3-14 shows the IV curve for a device with operating voltage as 5.5 V. The reason for different operating voltages still needs to be studied in detail, but it could be mainly due to the variation in the poly (EDOT-co-TAA) film in terms of % of TAA incorporation and overall thickness. With a new reactor being built in the lab with better design and ability to do in-situ thickness measurement, more desirable control on the

operating voltage of the devices may be possible and thus allow optimization of this layer for the improved working of the device.

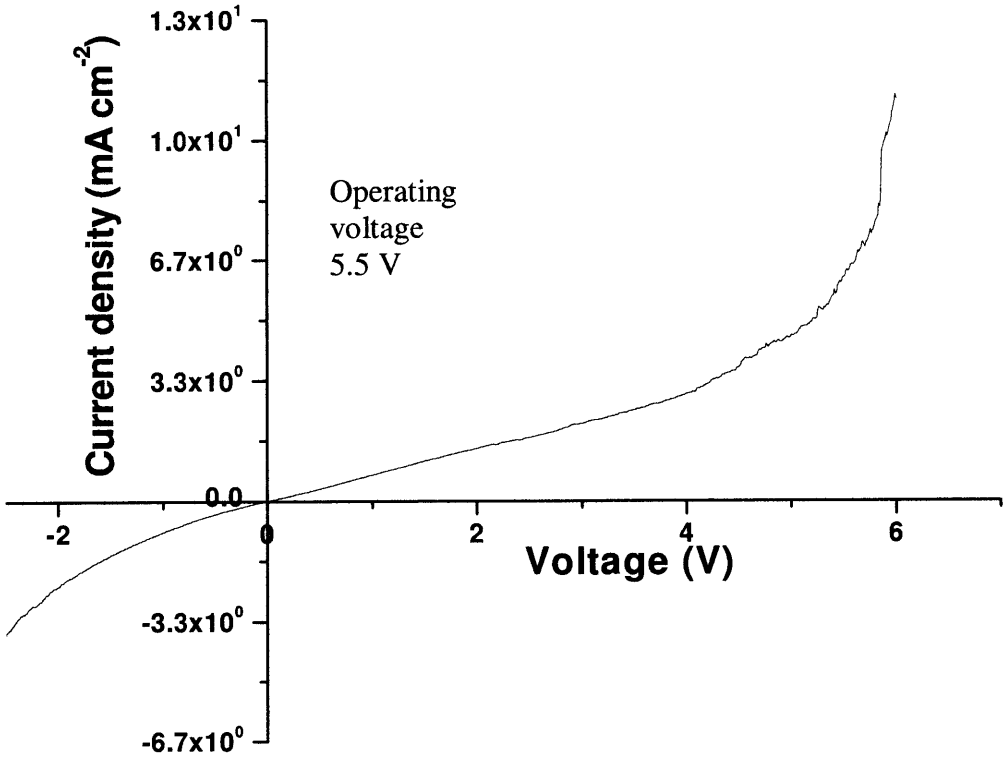

Figure 3-14: I-V characteristic of a working LED with operational voltage of 5.5 V.

3.3.2 Green Light Emitting Diodes

A few light emitting diodes with green light emitting QDs were manufactured. The advantage of this QD based HLED method is that for different colors, all the fabrication steps remain same and we only need to change the QDs used. Initial experiments with green light emitting diodes gave some exciting results but we still do not have a working green light emitting diode. The IV curve for the device in Fig. 3-15

shows diode characteristics but the current is very low, which is primarily the reason for not seeing any green light getting emitted on application of forward bias.

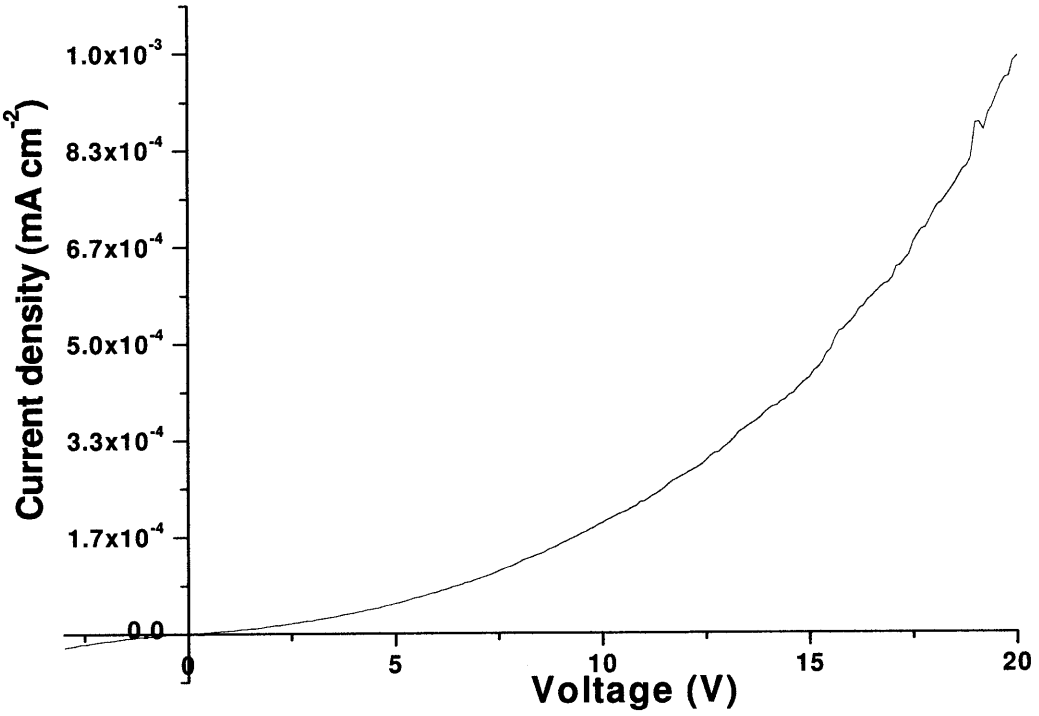

Figure 3-15: I-V characteristics curve for green QD-LED which showed diode behavior.

3.4 Stability

One of the issues with organic light emitting diodes is poor stability in air. Our preliminary experiments for the stability of red light emitting diode with operating voltage of 4.3 V show that the devices are very stable in air. Fig. 3-16 shows the IV curves for red light emitting diodes taken just after making device and after 10 days and 20 days. The IV curve obtained were very similar showing no or little degradation with time. It has to be noticed that device were stored in air and not in vacuum. No drop in the operating voltage was observed for the device.

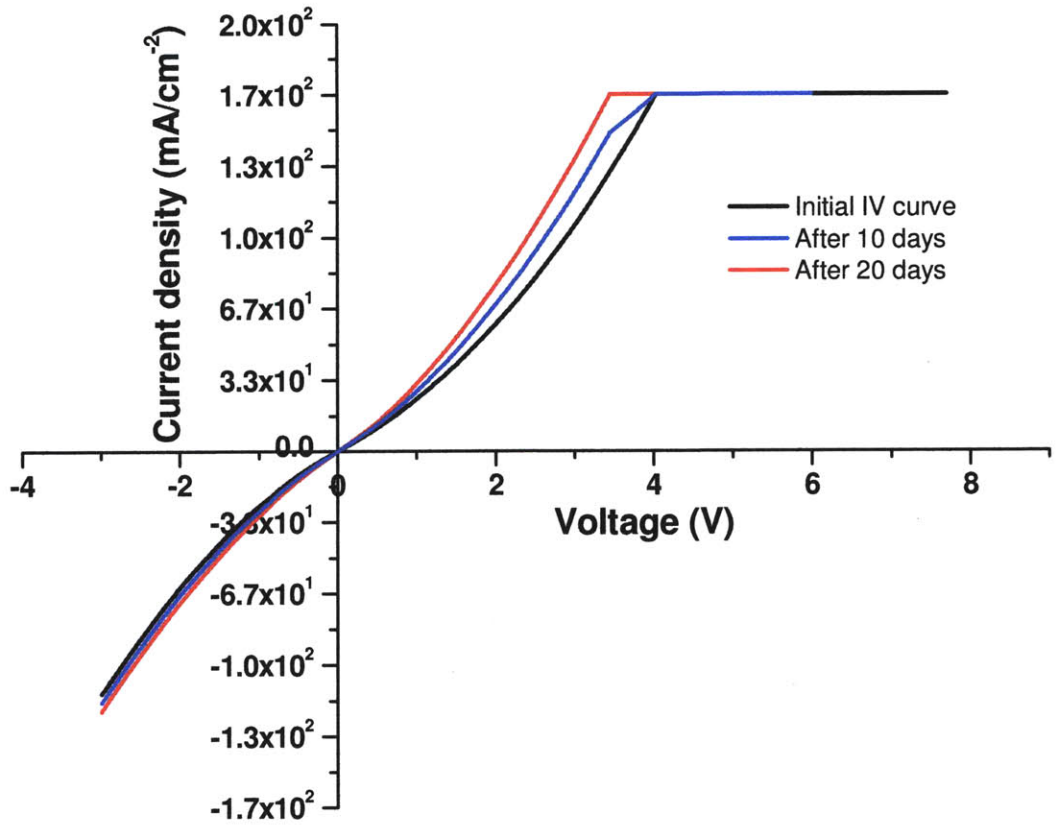

Fig. 3-16 I-V characteristics curve for red light emitting diodes with operating voltage of 4.3 V taken immediately after making the device and after storing the device in air for 10 days and 20 days, respectively.

3.5 Conclusions

The high color quality (saturated emission and tunable peak emission wavelength) of CdSe (ZnS) quantum dots distinguishes QD-LEDs over other technologies like OLED. But to be competitive in the LED market, improvements in QD-LED quantum efficiencies as well as demonstrations of long-lived QD-LED structures are necessary. In this work, we consider improvement in the stability of the HLED. The device fabricated can be configured as ITO/ poly (EDOT-co-TAA)/CdSe (ZnS)/ Au. All the materials used

in the device synthesis are stable in ambient conditions and all the synthesis steps after depositing electrode bilayers are done in air. This significantly reduces the cost of the device fabrication by obviating the need of packaging layers and ultrahigh vacuum tools.

Poly (EDOT-co-TAA) acts as the hole-transport layer in this device. This organic layer is stable in air and it might be possible to tune the work-function of this layer by oCVD process. Using diamine as a linker molecule to bind the –COOH functional group in the poly (EDOT-co-TAA), quantum dots were uniformly assembled on the substrate. The operating voltage as low as 4.3 V have been obtained for red-LEDs. We believe that with optimization of various layers in the device, further improvements can be made. For green LEDs, we obtained the characteristic IV curve of a diode, but we still need to work on getting a functioning green LED.

Acknowledgment

We would like to thank Deshpande Center for funding this research work. We would also like to thank Sreeram Vaddiraju for all his contributions in the project. Also, special thanks to Steven Kooi for helping in characterization of devices in ISN.

3.5 References

1. http://www.azom.com/Details.asp?ArticleID=4521
2. Schwartz, G.; Reineke, S.; Rosenow, T. C.; Walzer, K.; Leo, K.; *Advanced Functional Materials* 2009, 19, (9), 1319-1333.
3. Colvin, V. L.; Schlamp, M. C.; Alivisatos, A. P.; *Nature* 1994, 370, (6488), 354-357.
4. Gao, M. Y.; Lesser, C.; Kirstein, S.; Mohwald, H.; Rogach, A. L.; Weller, H.; *Journal of Applied Physics* 2000, 87, (5), 2297-2302.
5. Gao, M. Y.; Richter, B.; Kirstein, S.; *Advanced Materials* 1997, 9, (10), 802-810.
6. Huang, C. Y.; Su, Y. K.; Huang, T. S.; Cben, Y. C.; Wan, C. T.; Rao, M. V. M.; Guo, T. F.; Wen, T. C.; *2008 Ieee Photonicsglobal@Singapore (Ipgc), Vols 1 and 2* 2008, 258-260
7. Xing, K. Z.; Johansson, N.; *Advanced Materials* 1997, 9, (13), 1027
8. Do, L. M.; Han, E. M.; Yamamoto, N.; Fujihira, M.; *Molecular Crystals and Liquid Crystals Science and Technology Section a-Molecular Crystals and Liquid Crystals* 1996, 280, 373-378.
9. Aziz, H.; Popovic, Z.; Xie, S.; Hor, A. M.; Hu, N. X.; Tripp, C.; Xu, G.; *Applied Physics Letters* 1998, 72, (7), 756-758.
10. Do, L. M.; Oyamada, M.; Koike, A.; Han, E. M.; Yamamoto, N.; Fujihira, M.; *Thin Solid Films* 1996, 273, (1-2), 209-213.
11. Gautier, E.; Lorin, A.; Nunzi, J. M.; Schalchli, A.; Benattar, J. J.; Vital, D.; *Applied Physics Letters* 1996, 69, (8), 1071-1073.

12. Aziz, H.; Popovic, Z. D.; Hu, N. X.; Hor, A. M.; Xu, G.; *Science* 1999, 283, (5409), 1900-1902.

13. Do, L. M.; Han, E. M.; Niidome, Y.; Fujihira, M.; Kanno, T.; Yoshida, S.; Maeda, A.; Ikushima, A. J.; *Journal of Applied Physics* 1994, 76, (9), 5118-5121.

14. McElvain, J.; Antoniadis, H.; Hueschen, M. R.; Miller, J. N.; Roitman, D. M.; Sheats, J. R.; Moon, R. L.; *Journal of Applied Physics* 1996, 80, (10), 6002-6007.

15. Schaer, M.; Nuesch, F.; Berner, D.; Leo, W.; Zuppiroli, L.; *Advanced Functional Materials* 2001, 11, (2), 116-121.

16. Efros A1. L.; Rosen, M., *Annu. Rev. Mater. Sci.* 2000, 30, 475.

17. http://www.lumtec.com.tw.

18. Anikeeva, P. O.; Halpert, J. E.; Bawendi, M. G.; Bulovic, V.; *Nano Letters* 2009, 9, (7), 2532-2536.

19. Im, S. G.; Olivetti, E. A.; Gleason, K. K.; *Surface & Coatings Technology* 2007, 201, (22-23), 9406-9412.

20. Colvin, V. L.; Schlamp, M. C.; Alivisatos, A; *Nature* 1994, 370, (6488), 354-357.

21. Li, Y. Q.; Rizzo, A.; Mazzeo, M.; Carbone, L.; Manna, L.; Cingolani, R.; Gigli, G.; *Journal of Applied Physics* 2005, 97, 113501-1 - 113501-4.

22. Zhan, L.; Song, Z.; Zhang, J.; Tang, J.; Zhan, H.; Zhou, Y.; Zhan, C.; *Electrochim Acta* 2008, *53*, 8319-8323.

23. Vaddiraju, S.; Senecal, K.; Gleason, K. K.; *Advanced Functional Materials* 2008, 18, (13), 1929-1938.

24. Zhang, F.; Srinivasan, M.P.; *Colloids and Surfaces A: Physiochem. Eng. Aspects* 2005, 257-258, 509.

25. Bartlett, P. N., Dawson, D. H.; *J. Mater. Chem.* 1994, 4, 1805.

Chapter Four

Conclusions and Future Work

4.1 Oxidative Chemical Vapor Deposition of Conducting Polymers

Research on conducting polymers has been motivated by potential applications for flexible electronic devices. In this thesis we have successfully shown deposition of Poly (3, 4-ethylenedioxythiophene) (PEDOT) thin films through oxidative chemical vapor deposition (oCVD) by using a new oxidant- bromine. Previous oxidants used in this process like iron chloride or copper chloride required a rinsing by methanol to get rid of excess and reacted oxidant. The use of bromine eliminates any post processing rinsing step required and hence makes the process completely dry. On comparing properties of the films deposited using iron chloride and bromine as the oxidant, it is found that PEDOT films deposited with bromine have higher conductivity and conformality. Accelerated aging experiments also show longer retention of electrical conductivity for the PEDOT films obtained using bromine as the oxidant. All the results show the possibility of depositing highly conducting, conformal PEDOT films on any substrate including silicon, glass, paper, and plastic.

4.2 Development of QD based Hybrid Light Emitting Diodes

In this thesis, we have reported a technology to make hybrid light emitting diodes (HLED) which can potentially be employed to make efficient, cheap and stable LEDs with roll-to-roll processing. All the materials used in fabricating the device are stable in air and processing of materials after electrode bi-layer deposition is done in air. The configuration of the device fabricated is ITO/ Poly (EDOT-co-TAA)/ CdSe (ZnS)/Au. Poly (EDOT-co-TAA) is deposited using oxidative chemical vapor deposition process. CdSe (ZnS) is further attached to the ITO/Poly (EDOT-co-TAA) surface using a linker

molecule. Formation of conducting polymer was confirmed by Fourier Transform-IR. A photoluminescence spectrum indicates coalescence-free assembly of CdSe (ZnS) quantum dots with full width half maxima of 33 nm. Operating voltages as low as 4.3 V have been obtained so far and with further optimization of the device layers, we expect it to go below 4 V. Covalent interfacing resulting in enhanced charge transfer, low operating voltages and robust design along with the use of air stable materials for fabrication will result in HLED with improved performance and life. Preliminary results look promising for the development of air-stable and efficient HLED.

4.3 Future Work

To compete in the LED market, improvements in QD-LED quantum efficiencies as well as demonstrations of long-lived QD-LED structures are necessary. Technology developed in our lab after some improvements seems promising to make air-stable, efficient HLED. The current device configuration is ITO/ Poly (EDOT-co-TAA)/ CdSe (ZnS)/ Au and the lowest operating voltage obtained is 4.3 V. Some of the layers used in the device are not best suited for the improved working of the device. To identify the best materials for QD LEDs, it is necessary to look at the energy alignment of the ground and excited electronic states of QD monolayer and the surrounding organic thin films in a QD-LED. For HLEDs, the hole-transporting materials utilized have HOMO level at > 5 eV, so there is a significant potential energy step for the hole injection into the QD valence band positioned >6 eV below the vacuum level. The Au electrode used has work function of 5.1 eV, so there is a potential barrier for electron injection into the QD conduction bands that are between 4.0 and 4.8 eV below the vacuum level. The other

obstacle for electron injection (which is also a barrier for hole injection) into QDs is the insulating layer of organic ligands that are passivating the QD surface. But in reality the ligand layer is typically $\leq$0.5 nm thick, so it forms a minimal tunneling barrier for the carriers that pass through it.

The difference in potential barriers for hole and electron injection into QDs results in carrier imbalance at QD sites and formation of electron-exciton pairs that recombine via the Auger mechanism. These are the reasons for high operating voltages of current devices along with non-optimized thickness and work functions of various layers. Currently Au is being used as an electrode but its energy work function is not best suitable for the device. This results in a barrier for injection of electrons from metal electrode. Using other electrodes like Mg/Ag with lower work functions will help in reducing the operating voltage. Also, use of an electron-transporting layer like P3HT will help in reducing the operating voltages and leakage current. And once efficient red light emitting devices are obtained, efforts should be diverted to develop green and blue light emitting diodes.

Also, we have shown that the PEDOT deposited using bromine have higher conductivity and show better retention of conductivity under accelerated aging conditions. To improve the life time of the LEDs, it will be worthy depositing poly (EDOT-co-TAA) films using bromine as the oxidant and study its electrical properties. Higher conductivity of hole-transporting layer will reduce the hole injection barrier and hence will reduce the operating voltage and at the same time better stability of the HTL film will improve the life time of the device.

Future work should be done in studying the electrical properties of the PEDOT films deposited using bromine and possible applications of the films in devices like solar cells and light emitting diodes. Grafting of oCVD PEDOT on polymer substrates has already been shown so it is possible that oCVD PEDOT deposited using bromine can play a unique role in flexible electronics.

Appendix A

Experimental Details for QD based LEDs

A.1 Experimental Details for QD based LEDs

Step1
Substrate Preparation
1) Ultrasonicate substrates in Micro 90 with DI water for 5 mins.
2) Rinse it with water (USE ONLY DI WATER)
3) Ultrasonicate with Isopropanol for 5 mins (Make sure no carbon residues are thr and then clean with pressurized air)
4) Rinse with DI water (DO ONE MORE ISOPROPANOL FINAL CLEAN)
5) Clean with air gun and check which side has ITO

Step 2
Etching off substrate
1) Put scotch tape on sides and press with rubber (PUT TWO LAYERS OF TAPE OTHERWISE IT WILL COME OFF)
2) Etch off with sulphiric acid and hydrogen per oxide (50/50 soln) by dipping for 5 mins
3) Clean with water and Isopropanol
4) Check for conductivity (MAKE SURE THE REGION BETWEEN THE ITO STRIPS IS GONE)

Step 3
Chemisorption of 3-TAA
1) Dip in solution of 3-TAA in methanol (USE 30 MINUTES), PRIOR TO THIS, CLEAN USING OXYGEN PLASMA for 15 min

Step 4
OCVD deposition of poly(PEDOT-co-TAA)
1) Put scotch tape on sides leaving space for ITO contact, we put silver paste on ITO for better results
2) Conditions :-TAA (monomer #2)- 180 C, Substarte - 80C, EDOT- 150 C, Iron Chloride in Excess
3) Deposit for 15-20 mins
4) If appearance is hazy it means we have TAA
5) Remove PEDOT-TAA from center
6) Use methanol and cotton tips for edges(Use separate cotton tip for each edge)
6) Check conductivity through multimeter

Step 5
Attaching di-amine Linker
1) Prepare 3 solutions in DI water of PDA, NHS, DCC(in refrigerator) and ultrasonicate for 5 mins (BUY FRESH DCC, get small quantities and throw them away after few weeks). PDA use for one month and then buy new.
2) In one container take 2-3 ml of NHS, DCC and excess of PDA and keep it in solution for 1 hr.
3) Take out the substrate and clean with DI water

Step 6
Attaching Quantum Dots
1) Make NHS and DCC solution again

2) Make QD solution (1 ml of QD as-obtained from N,N labs in 50 ml water and make solution of 4-Mercaptobenzoic acid in water (0.0001 m) and ultrasonicate for 1 hr). Keep this soution for 2 days. Other option is to directly use the as obtained QD and dilute it.

3) Put substrate in NHS and DCC solution and add 8 ml of QD solution (HERE, use very small amounts of
DCC and NHS, 1 ml each only), make sure the substrate is completely nsubmerges in the solution, else, add a few ml of pure DI water

4) Keep the solution for 1 day and protect it from light by wrapping with Aluminum foil

Step 7
Gold deposition
1) Put mask and deposit gold (10 A current for 50 sec, 25 A for 50 sec, 45 A for 100 sec)